DESIGN OF CHIP RESISTOR LOADED METAMATERIAL BASED ELECTROMAGNETIC STRUCTURES

A thesis submitted in Partial Fulfilment of the Requirement for the Award of the Degree of

MASTER OF ENGINEERING

In

Wireless Communications

Submitted by

Tanveer Kaur Suchu

Roll No. 801563027

Under Supervision of

Dr. Rajesh Khanna
Professor, ECED

Dr. Ravi Panwar
Assistant Professor, ECED

ELECTRONICS AND COMMUNICATION ENGINEERING DEPARTMENT

THAPAR UNIVERSITY, PATIALA, PUNJAB

JUNE, 2017

DECLARATION

I Tanveer Kaur Suchu hereby declare that the work presented in this thesis entitled "DESIGN OF CHIP RESISTOR LOADED METAMATERIAL BASED ELECTROMAGNETIC STRUCTURES" is fulfilment of the requirement for the award of degree of Master of Engineering submitted at Electronics and Communication Department, Thapar University, Patiala is an authentic record of work carried out under supervision of Dr. Rajesh Khanna (Professor, Department of ECE, Thapar University) and Dr. Ravi Panwar (Assistant Professor, Department of ECE, Thapar University) from 2015 to 2017. The matter presented in this has not been submitted either in part or full to any other university or institute for the award of any other degree.

Date..14th July'17.

Tanveer Kaur
801563027

It is certified that the above statement made by the candidate is correct to the best of my knowledge and belief.

Date:..14th July'17...

Dr. Rajesh Khanna
Professor
ECED

Dr. Ravi Panwar
Assistant Professor
ECED

i

ACKNOWLEDGEMENT

While bringing out this thesis to its final form, I came across a number of people whose assistance in a variety of ways helped my field of research and they ought to have special thanks. It is a pleasure to convey my thankfulness to all of them.

I would like to express sincerest gratitude to my esteemed mentor **Dr. Rajesh Khanna, Professor**, and **Dr. Ravi Panwar, Assistant Professor,** Electronics and Communication Engineering Department, Thapar University, Patiala, for their regular devotion and valuable guidance throughout the completion of the dissertation. It has been a matter of privilege to get the opportunity to learn great insights of in-depth knowledge under their mentorship.

I would like to thank **Dr. Alpana Aggarwal, Professor and Head**, Electronics and Communication Engineering Department, Thapar University, for her earnest efforts to inspire the students to perform efficiently to meet the research objectives.

I express gratitude to **Dr. Hemdutt joshi, Associate Professor and P.G. Coordinator**, Electronics and Communication Engineering Department, Thapar University for inspired motivation to give the best of the potential at each step.

I am highly grateful to all of the seniors and faculty supervisors for being essential motivators to achieve the objectives of the course of Masters in Engineering.

Next, I gave my sincere thanks the authors from the research community whose work has been greatly encouraging and has been duly quoted as reference in the thesis report.

Last but not the least I, heartily thank Almighty and my parents for their consistent blessings and support.

ABSTRACT

Due to the unique electromagnetic (EM) characteristics, metamaterial structures (MMSs) have achieved increasing attention of the researchers. MM are the artificial periodic structures with lattice constants that are much smaller than the wavelength of the incident radiation. Therefore providing negative refractive index characteristics. A wideband MMSs using traditional and Nature Inspired (NI) Conducting Geometries (CG) loaded with lumped resistor have been designed in the range of 2 to 18 GHz. The MMS consists of a resistor loaded CG, a dielectric sheet and a metallic ground.NI –CGs can be employed for the fulfilment of broadband absorption due to its attractive features like space-filling, multiband resonance, and self-similarity. The EM characteristics of NI-CGs depends on CG shape, CG iteration order and dielectric constant of the substrate. Moreover, an incorporation of chip resistors can further improve the reflectivity characteristics of NI-CG based MMSs.

The results show that the MMS covers the wide frequency range with reflection loss below -10 dB at normal incidence. The broadband absorption is mainly resulted from the strong EM resonance. The obtained result reflects the potential of lumped resistor based MMSs for distinct EM applications. Various shapes of CG analysed and their complexity have been taken into account in order to improve the S_{11} characteristics. Efforts were made in order to design the MMSs for low frequency applications by inserting spacer foam in between the dielectric substrate layer and the conducting sheet. Different physical parameters are studied for these geometries, and the working mechanisms behind these phenomena are explained in this thesis. Some potential applications of these structures are also discussed. The purpose of this study was to develop new CG based MMS designs to maximize the bandwidth of structure. A Triple Square (TS) -MMS structure is found to accomplish more extensive peak RL value with wide bandwidth when contrasted with NI-CGs.

CONTENTS

Sr. No. **Page No.**

LIST OF FIGURES

.

LIST OF TABLES

LIST OF ABBREVIATIONS

MMS	Metamaterial Structure
EM	Electromagnetic
NI	Nature Inspired
CG	Conducting Geometry
PEC	Perfect Electric Conductor
DPS	Double positive
ENG	Epsilon negative
DNG	Double negative
MNG	Mu-negative
RH	Right Handed
TL	Transmission Line
LH	Left Handed
MM	Metamaterial
ITO	Indium tin oxide
CM	Chiral Media
CP	Circularly Polarized
CMM	Chiral Metamaterial
NRI	Negative Refractive Index
EMI	Electromagnetic Interference
EMC	Electromagnetic Compatibility

FWHM	Full Width at Half- Maximum
FG	Ferrite-Graphene
AFSS	Active Frequency Selective Surface
HIS	High-Impedance Surfaces
TM	Transverse- Magnetic
TE	Transverse- Electric
RCS	Radar Cross-Area
MAM	Microwave Absorbing Material
GA	Genetic Algorithm
EBG	Electromagnetic Band Hole
PBG	Photonic Band Hole
LRE	Lumped resistor element
RL	Reflection Loss
TS	Triple Square
DS	Double Square
SS	Single Square

CHAPTER 1

INTRODUCTION -+

On the order of the angstroms, natural substances are different from various atoms and molecules. When there is interaction between natural materials and visible light, then standard processes such as transmission, reflection and absorption follows the presumed behavior. This is because the visible light wavelength is multiplied in comparison to atoms and molecules of component[1]. At a basic level, standard length of unit cell controls the absorption, reflection, and transmission of the molecule.. Artificially made structures are known as (MMSs) metamaterial structures where the unit cell is designed with length for the particular specifications. The expression "artificial" alludes towards a way that the EM reaction for such kind of materials governed by the scattering and are placed periodically in corporations (e.g. cut wires, Metallic loops or dielectrics0) with a trademark have medium. The expression "extraordinary" suggests that EM reactions of those materials are not observed in nature. Without a doubt, above mentioned property is the wellspring of the prefix Meta, in Greek it means "past" 'a great many'. As said before in the discussion, metamaterials give electromagnetic (EM) properties not easily accessible in nature[2]. This makes them exceptionally valuable, useful and interesting for an extensive variety of microwave applications, going from minimal stage shifters to productive antennas. In view of the previously mentioned valuable properties of metamaterials, it was chosen to examine metamaterial structures for three firmly related applications: absorbers, artificial plasmonic structures, and cloaks. In planning metamaterials, periodic array of unit cellsis carefully engineered to make an artificially organized composite material. Metamaterials help to get free from the limitations of normally happening materials and take into consideration full control over light flow through the outline of artificial materials. These unit cells consist of constituent components with periodicities running from several nanometers to millimeters contingent upon the objective specific frequency, and in this way are considerably bigger than the molecular or atomic scale includes that are normal in natural materials. Cautious outline of every unit cell and the periodicity of a metamaterial empowers a wide assortment of new material properties. The capacity to decouple the optical properties of an outfit through the cautious assembly of its constituents prompts a wide variety of new gadget plans and applications. For miniaturization and optoelectronics of optical segments, various gatherings have exhibited novel sorts of optical modulators and filters. Materials with negative refractive index could give a path to the design of perfect lenses wiping out the limits of resolution by diffraction.

Recently, the capacity to make optical cloaks has additionally attracted a significant measure of consideration. This has been accomplished at microwave frequencies utilizing transformation optics, a specific branch of metamaterial research, and depends not on negative index materials yet rather on the capacity to independently build the optical properties of every unit cell over a surface.

While metamaterials might be intended to alter various properties, we will concentrate on electromagnetic metamaterials that affect the properties of the incident electromagnetic waves. Specifically, sub-wavelength metallic components support sharp resonances, and we plan composites in view of metallic structures to tune the reaction of incident light. Keeping in mind the end goal to correctly comprehend what metamaterials are and how to outline them, we will first consider the general reflection properties that define all materials [1].

1.1 HISTORY AND BACKGROUND

Metamaterials appeared later (five decades) after the Second World War. The acknowledgment of artificial materials begun toward the end of the nineteenth century (1898) when Jagadis first played out his analysis on wound structures' geometries which was essentially an artificial component called chiral as the present time scientists call it. Right on time in the twentieth century (1914), Lindell et al. made a chiral medium by embedding a few arbitrarily situated little wire helices in a host medium [3]. In this manner, in 1948, Kock additionally composed a lightweight microwave focal point by controlling the leading circles, time frame strips and also fitting the compelling refractive file of the fake media. Because of the progression in the study of materials, more engineered materials were created which exhibited whimsical properties. It is Veselago's tempting guarantee of negative list materials at optical frequencies that has driven a significant measure of work in the metamaterial field. Throughout the most recent decade, the principle drive in metamaterials research was to drive the research of artificial materials to ever higher frequencies with a definitive objective of making materials in the visible part of the range. It is a fortuitous situation that this drive was reflected by significant advances in nanofabrication instruments [1]. These apparatuses made it conceivable to create as well as test and configuration structures with resonant properties from the microwave through the close IR. In 2007, Soukoulis et al. distributed an article depicting how the resonant reaction of metamaterials had been pushed from microwave, where the unit cell is on the request of millimeters, to noticeable wavelengths, where to be sub wavelength metamaterial unit cells must be at the request of 100 nm in size. The path to clearly visible wavelength, in any case, revealed the limitation of the split ring design i.e. size limitation. This limitation is a

consequence of the way that metals don't work as perfect conductors in the visible range. This incited a move from SRR-based metamaterials to cut wire sets to fishnet structures.

1.2 MOTIVATION

In the 1960s, there was an incredible stimulus towards the acknowledgment of 'artificial dielectrics'. These works looked to synthesize effective materials with electromagnetic scatters, which could be intended to deliver a specific plainly macroscopic response at long wavelengths. As said before in the discussion, metamaterials give electromagnetic qualities not promptly accessible in nature. This makes them extremely intriguing and valuable for an extensive variety of microwave applications, going from reduced phase shifters to proficient antennas. In light of the previously mentioned valuable qualities of metamaterials, it was chosen to research metamaterial structures for three nearly related applications: safeguards, shrouds, and simulated plasmonic structure. As of late, artificial dielectrics have encountered a resurgence of enthusiasm under the pretense of metamaterials. Extensively, metamaterials are artificial dielectrics with otherworldly electromagnetic properties. One of the inspirations for creating metamaterials is to accomplish relative electric permittivity (ε_r) and attractive permeability (μ_r), in the regimes not promptly accessible utilizing naturally available materials. Additionally, expanding the refractive record over a substantial frequency regime brings about broadband moderate light, which can be utilized to improve the capacity limit of delay lines and in addition spectral affectability in interferometers. Here we design a three-dimensional metamaterials structure with a refractive index that is subjectively low and non-dispersive, over an expansive frequency regime. Rather than our work, past ways to deal with improving the refractive index used either electronic resonances in atoms or electromagnetic resonances, for example, split-ring resonators. These plans are intrinsically narrowband and work just in the region of a resonating frequency. Identified with our work, it was found that the utilization of a variety of chip resistors could prompt the frequency dependent and broadband enhancement of bandwidth and the relative electric permittivity ε_r. We aim at designing novel metamaterial structures and use them further to improve the characteristics of MMSs. This will give more design freedom and a better performance for various applications

1.3 KEY OBJECTIVES

The main objective of this thesis is to explore advanced MMSs with broadband absorption characteristics in the range of 2 to 18 GHz. The following major tasks have been accomplished in this thesis:

- To examine the effect of aperture and patch geometries over reflection loss characteristics of MMS.
- To investigate chip resistor loaded broadband MMSs and to examine the effect of variation of dielectric constant, substrate thickness, spacer layer thickness and resistance value.
- The design of nature inspired MMSs loaded with chip resistors and to study the effect of higher iterated geometries, spacer thickness, dielectric constant, dielectric thickness and resistance over S_{11}.

1.4 STRUCTURE OF THE THESIS

Chapter 1 discusses about the basic introduction and background to the MMSs as a rapidly growing field in MM research. Chapter 2 briefly discusses about the literature review on traditional MMSs, resistor loaded MMSs and nature inspired (NI) MMSs.Chapter 3 is dedicated to the effect of the patch and aperture geometry followed by the resistor loaded conducting geometries (CGs) and their parametric analysis.Chapter 4 describes about the effect of the NI-CGs based MMSs with detailed analysis on the dielectric constant, dielectric &spacer thickness and resistance values. Finally in chapter 5 conclusions and the potential for future work is described.

1.5 APPROACHES UTILIZED

In this thesis, an efficient design has been presented for obtaining the wide band absorption in the range of 2 to 18 GHz. The following approaches have been utilized to achieve this task:

A) DESIGN OF TRADITIONAL MMS

In this thesis, we begin to design our unit cell MMS using commercially available software CST MICROWAVE STUDIO SUITE. It is a complete features software package used for EM designs and analysis in the high-frequency range [7]. This software consists of several techniques for the simulation process such as frequencyand time domain solver, multilayer and asymptotic solver, Eigen mode and integral equation solver. These techniques are best suited for various applications. CST is best suited for efficient, simple or complex design

and analysis of the components like filters, connectors, couplers, antennas, resonators and may more. Since the underlying method is for 3D approach, this software can solve any high-frequencyfield problem. It's possible to achieve perfect absorption only when the reflection at an interface can be completely eliminated. As it is hard to coordinate the impedance matching between free space and an absorbing material, MMSs utilizes an alternative approach by taking advantage of interference and multi reflection. MMSs design consists of a metal ground plane and a thin dielectric layer separated by a dielectric spacer. The incident electromagnetic wave is therefore completely dissipated in the resistive screen and trapped in the structure. However, they restrict their use in many applications as they are bulky and operate over a narrow bandwidth. Broadening the bandwidth can be achieved by using multi layered and lumped elements in the structures. The top sheet not only contains a resistive component but is also reactive, by using conducting geometries loaded with the resistors.

STEP I: Perfect Electric Conducting Layer (PEC)

In our design, initially, theperfect conducting layer is considered as shown in figure 1.1. A perfect conductor or perfect electric conductor (PEC) is a perfect material revealing equivalently, zero resistivity or infinite electrical conductivity. Perfect electric conductors are used because they have zero electrical resistance. Within PEC there is a steady current flowing which flows without dissipating any of its energy to the resistance. Since there is no loss of energy to resistance and resistance is responsible for heat generation, there will be no dissipation of current eventually no heat generated inside PEC. Current will indefinitely flow inside PEC until no potential difference exists.

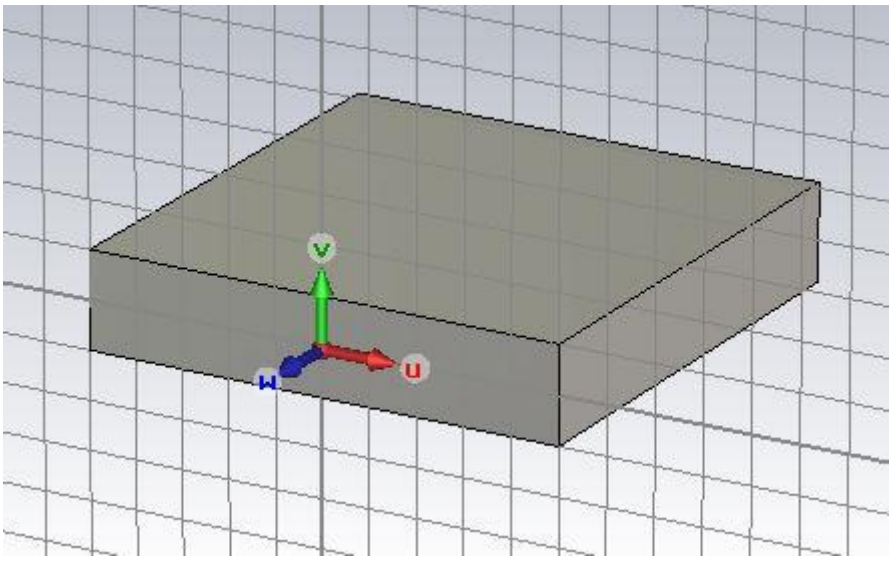

FIGURE 1.1. 10 × 10 mm Perfect Electric Conducting (PEC) layer.

STEP II: Dielectric Substrate layer

Any electrical insulator possessing property to get polarized by applying an electric field is known as dielectric layer/material shown in figure 1.2. At the point when a dielectric is set in an electric field, electric charges don't move from the material as they do in an electrical transmitter, however there is somewhat movementin their normal balance locations causing dielectric polarization. In view of dielectric polarization, negative charges moves away from the field whereas the positive charges move the other way. This leads to the inner E field that diminishes the overall field present in the dielectric itself. Dielectric properties play a major role in changing the absorption bandwidth properties so to observe that we tried to change the dielectric values in our design. Generally following dielectric constant values are used for the purpose. In this thesis, primarily study has been carried out over low dielectric constant value.

TABLE 1.1 MATERIAL AND THEIR DIELECTRIC CONSTANT VALUES

MATERIAL	DIELECTRIC CONSTANT VALUE
ROGERS	2.25
FR-4	4.3
ARLON 1000	10
GALLIUM ARSENIDE	12.9

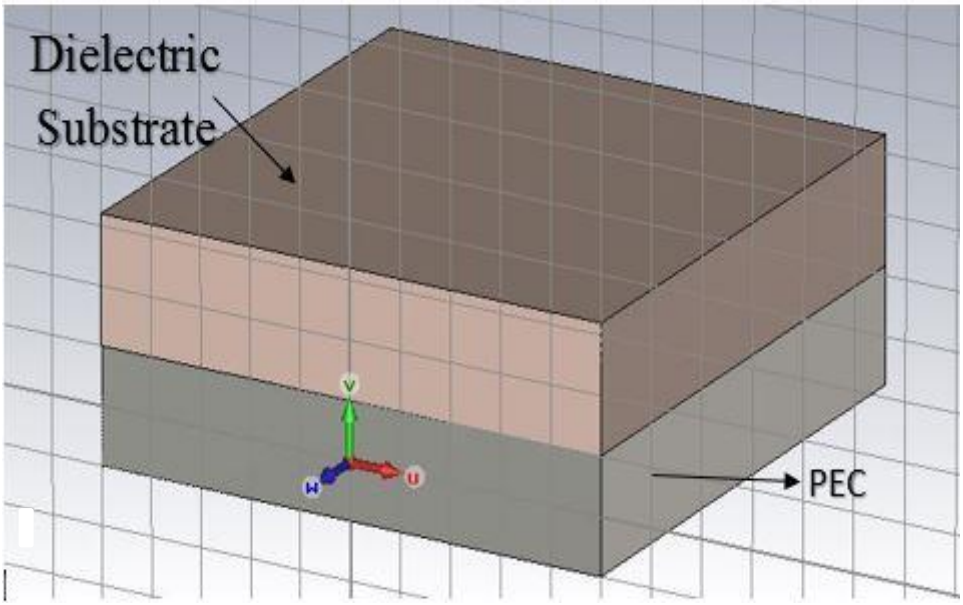

Figure 1.2. Dielectric layer placed over 10 × 10 mm PEC

STEP III: Conducting geometry imprinted on the dielectric layer.

Conducting geometry is repetitive structures primarily outlined to transmit, absorb and reflect EM fields over the certainrange of frequency as depicted in figure 1.3. They are constructed by printing periodic metallic patterns either on a single side or both sides of a dielectric substrate. To excite any MMS we need to set the periodic boundary conditions and the available ports. For excitation, various ports such as waveguide port, discrete port or floquet ports can be used. In our design, the realization of conducting geometry based MMSs floquet theory is used. Similarly, various conducting geometries can be used as shown in figure 1.4.

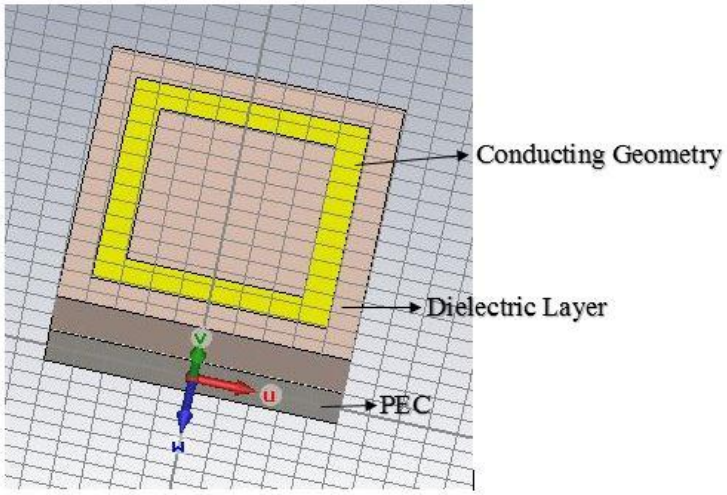

Figure 1.3. Conducting geometry imprinted on dielectric layer

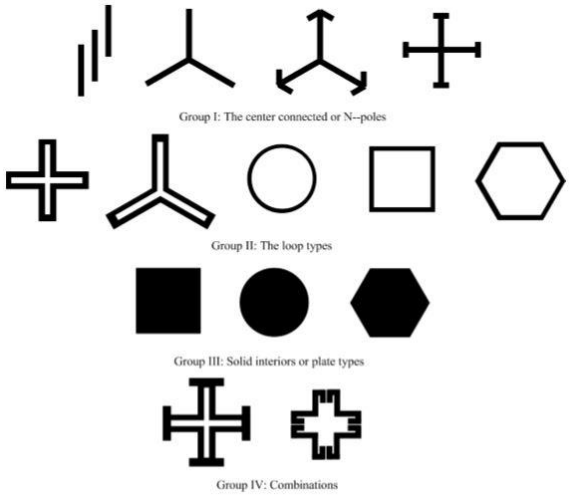

Figure 1.4. Various traditional conducting geometries [6].

The Floquet port in CST is utilized only with planar- periodic structures [7]. Primary examples are conducting geometries and phased array when these might be idealized as infinitely large. The examination of the infinite structure is then refined by investigating a unit cell. Often the side walls of the unit cell are formed by the linked boundaries, but

additionally in order to represent the infinite space at least one open periodic boundary condition are needed. Sometimes radiation boundaries have been used. The Floquet port is another alternative. Floquet ports are shown in Figures 1.5 (a) and (b):

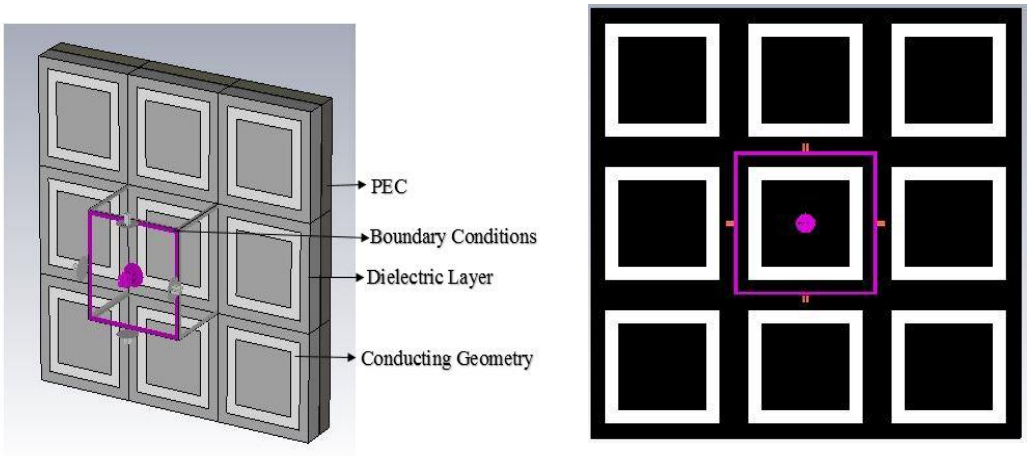

Figure 1.5. Floquet ports applied on the MMSs a) Side view b) Front view

B) DESIGN OF CHIP RESISTOR LOADED MMS.

STEP I: Initially PEC layer is considered as already discussed above.

STEP II: The spacer layer between dielectric substrate and PEC layer

Spacer plays a major role in increasing the S_{11} characteristics of the structure. Therefore initiative has been taken to consider the spacer layer in between the dielectric and PEC layer as shown in figure 1.6.

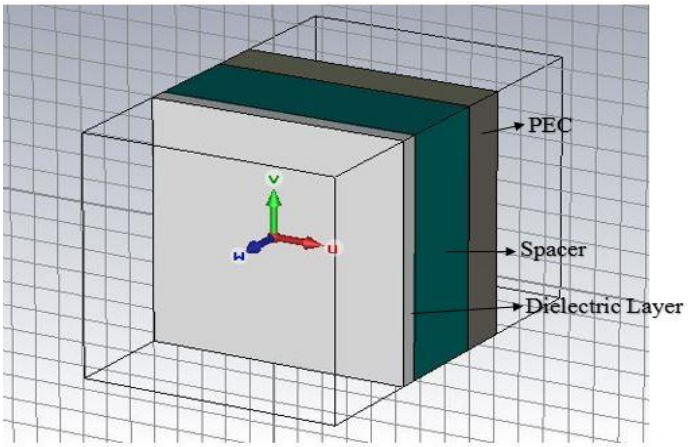

Figure 1.6. Spacer layer inserted between dielectric and conducting layer

STEP III: DIELECTRIC LAYER OVER SPACER: This step has been discussed earlier in the previous section.

STEP IV: Resistor loaded conducting geometry imprinted on the dielectric layer.

As discussed earlier the Floquet theorem has been utilized in order to develop periodic EM structures and accordingly the unit cells with size 10 mm × 10 mm has been utilized as shown in figure 1.7(a). Implication of the boundary conditions are vital to the MMSs in determining the model scope,truncating the infinite space to finite volume and they can also help in reducing the transmission time and computation demands. In this thesis, periodic boundaries are applied to provide periodicity to the unit cell MMSs as shown in figure 1.7(c). In this step passive elements, i.e. resistors are loaded in the conducting geometry to enhance the S_{11} properties. The embedded resistors can also consume some portion of the EM energy and thus realizing the increased bandwidth

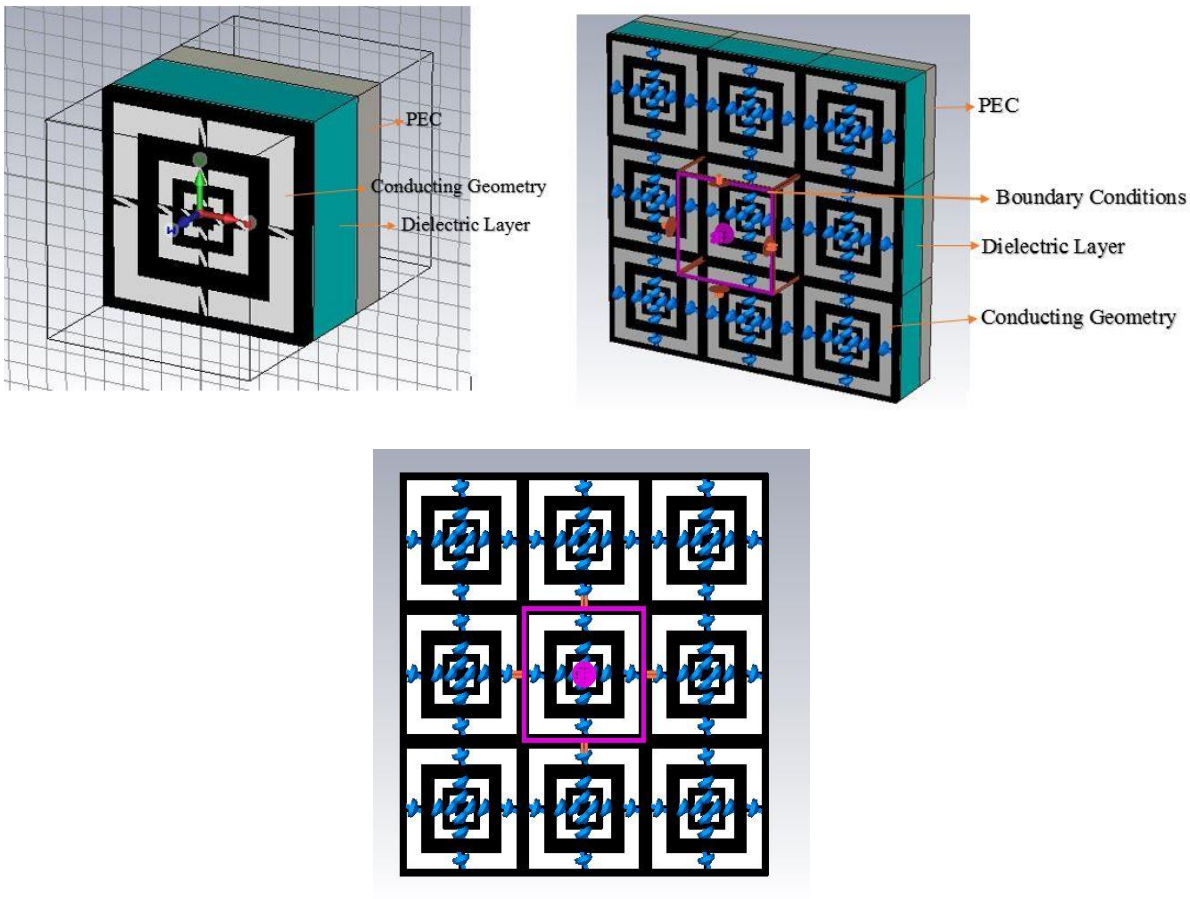

Figure 1.7. Resistor loaded MMSs a) side view b) Floquet port side view c) Floquet port front view.

C) DESIGN OF NATURE INSPIRED MMS LOADED WITH RESISTORS.

In order to improve the absorption bandwidth issues, nature inspired based conducting geometry have been adopted as shown in figure 1.8 (a). Nature inspired shapes topossess an interesting property, i.e. the self-similarity property. Briefly speaking, when there was the replication in the geometry of MMSs, self-similarity can be described. In self-similarity property, the geometry of the structure has been scaled at different levels within that same

original structure. Thus, wideband and multiband behaviour were the results of the self-similarity of nature inspired structure. In the previous years, various conducting geometries such as multipole, the multiband and band stop were successfully designed and fabricated using the nature inspired shapes. For simulation process, similar boundary conditions (floquet ports) are used as shown in figure 1.8 (b).

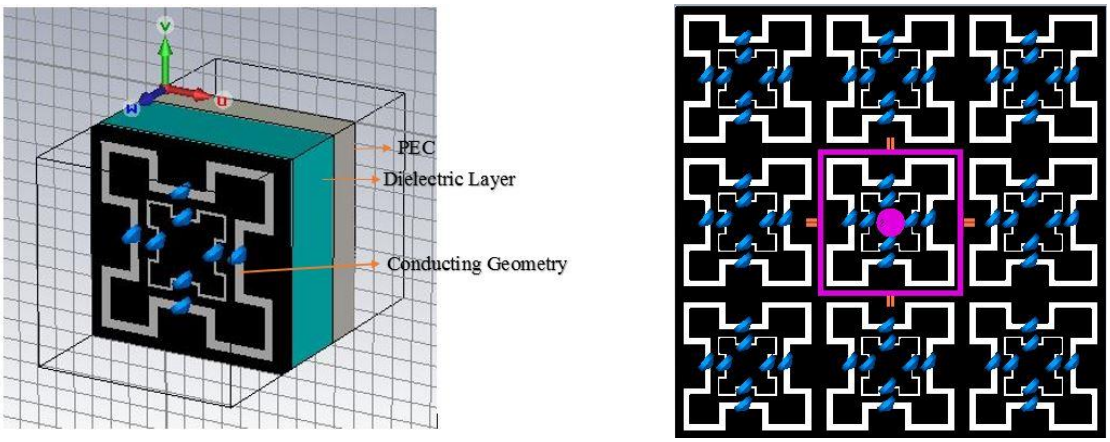

Figure 1.8. Nature inspired MMS (a) Side view b) Floquet port side view.

CHAPTER 2

LITERATURE REVIEW

2.1 INTRODUCTION

The prior work done in the field of advanced EM structures have been investigated. Based on the permittivity and permeability values. The EM structures can be classified as Double positive (DPS), Epsilon negative (ENG), Double negative (DNG) and Mu-negative (MNG) materials as shown in figure 2.1.The materials with positive permeability, permittivity and refractive index, i.e. $\mu > 0$ and $\varepsilon > 0$, are presented as DPS. These dielectric materials naturally exist lying in quadrant–I. The direction of wave vector and the Poynting vector in these materials is same. These are also known as right-handed materials. Epsilon negative (ENG) materials such as metals and plasmas at optical frequencies are examples of materials belonging to quadrant–II where $\varepsilon < 0$, $\mu > 0$. Quadrant–III materials having the property of permeability and permittivity as ($\varepsilon < 0$, $\mu < 0$) as well as a negative refractive index is known as left-handed materials or DNG materials. Their existence is not there in nature. These materials are in opposite directions for Poynting vector and wave vector. Mu-negative (MNG) materials ($\varepsilon > 0$, $\mu < 0$) like gyrotropic and ferromagnetic materials belong to the quadrant.

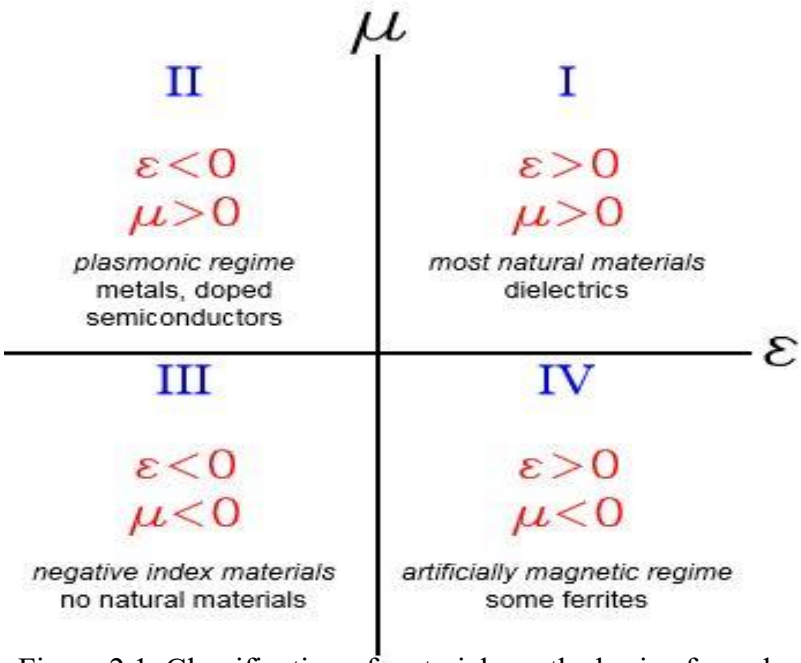

Figure 2.1. Classification of materials on the basis of ε and μ [8].

2.1.1 RIGHT HANDED (RH) MMS

Figure 2.2 shows a 2 dimensional propagation in RH medium represented by unit cell (having length d) loaded with lumped component. It is nonmagnetic, isotropic and possess a relative permittivity ε_r holding their developing frequency dependency in the documentation for keeping the generality $\mu(\omega) = \mu_0$, $\varepsilon(\omega) = \varepsilon_r\varepsilon_0$according to $Z' = j\omega\mu_0 g$ and $Y' = j\omega\varepsilon_r\varepsilon_0/g$ [8]. Here the two comparing distributed properties are $L_0 = \mu_0 g = L/d$ (H/m) and $C_0 = \varepsilon_r\varepsilon_0/g = C/d$ (F/m), where both of them are real and positive [9]. Proposed model expects zero losses, still it is possible that losses are undoubtedly added in the run of the typical Transmission line (TL) sense, i.e., possessing a conductance for shunt & resistance for series connection. Considering the same limit, when $d/\lambda \rightarrow 0$,the comparing propagation consistent β is obtained by using the circuit wave condition,

$$\frac{\partial^2 V_y}{\partial x^2} + \frac{\partial^2 V_y}{\partial z^2} + \beta^2 V_y = 0, \qquad \beta = \pm\sqrt{-Z'Y'} \tag{2.1}$$

On reducing to the standard TL, filled with a nonmagnetic dielectric with relative permittivity ε_r[9],

$$\beta = \pm\sqrt{-Z'Y'} = \omega\sqrt{L'C'} = \omega\sqrt{\mu_0\varepsilon_0\varepsilon_r} \tag{2.2}$$

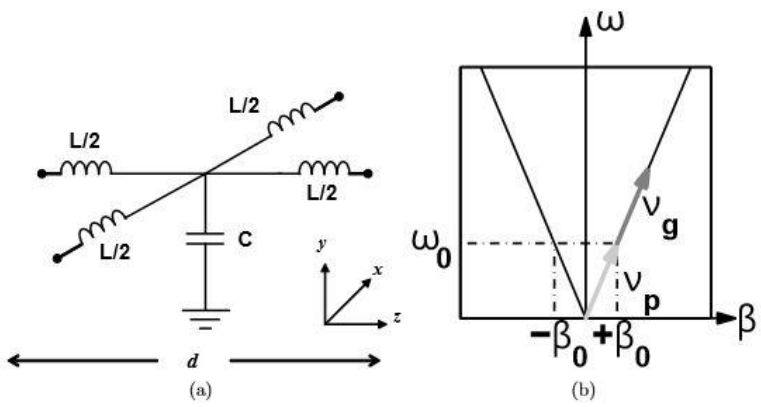

Figure 2.2. a) 2D TL unit cell, b) propagation for dispersion relation in particular in x-z plane [10].

The decision of the positive root builds up the tradition that the group speed is positive, which guarantees that power flows away from the source. The ω–β bend or subsequent scattering connection, depicts variety of the propagation constant along a specific axis of propagation in the x–z plane as a component of frequency, as appeared in Fig. 2.2 (b). The ω–β bend can be used to surmise the magnitude of the group velocities and phase present in the medium. The

group velocity can be is expressed as Vg = ($\partial\beta/\partial\omega$) − 1, which is the slope of the tangent to the ω–β bend at (ω_0, β_0) and the phase velocity is expressed as the proportion vφ = ω/β, where magnitude can be defined with the incline of a line for the ω–β bend till a point (ω_0, β_0).

It's obvious from Fig.2.2 (b) that the shunt capacitance and series arrangement inductance helps in displaying the propagation constant of traditional isotropic RH medium. It fluctuates relatively with frequency, as would be normal at low frequencies in regular dielectrics. It is additionally evident that the subsequent group velocities and the stage are parallel and equivalent and are given by [11]:

$$\upsilon_\varphi = \frac{\omega}{\beta} = \sqrt{\frac{1}{L'C'}} = \sqrt{\frac{1}{\mu\varepsilon_0\varepsilon_r}} = \upsilon_g \tag{2.3}$$

Positive phase velocity implies that there is a phase lags towards the group velocity direction in RH media. In this manner, the refractive index, expressed as the proportion between the phase velocity and the speed of light in a vacuum, is positive [12].

$$n = \frac{c}{\upsilon\varphi} = \frac{\sqrt{L'C'}}{\sqrt{\mu_0\varepsilon_0}} = \sqrt{\varepsilon_r} \tag{2.4}$$

2.1.2 LEFT HANDED (LH) MMS

Metamaterials as the built materials are produced using a course of artificial unit structures ("metal-particles/metal-atoms") which are formed from officially existing substances and organized in periodic shape. The combination of those unit structures frames another material which shows uncommon properties not quite the same as its elementary constituents. Subsequently, the reaction of a metamaterial structure to the electromagnetic wave and its conduct depend totally on the MM unit cell (composite materials and their plan in a unit cell). Therefore, when outlining metamaterials, the choice of materials to utilize and their physical properties (Optical and electronic properties) should be all around considered with a specific end goal to comprehend the reasonable material for the planned design, application and the wavelength range of intrigue. Fundamentally, in gadgets, there are three sorts of materials: conductors/metals, dielectrics/insulators, and semiconductors.

These material arrangements are grounded in their conductivity qualities which are clarified by energy band structure or electronic energy levels. Electronically every material comprises of two fundamental energy groups; valance and conduction groups isolated by a void space. The conduction band is at the highest energy level and generally void, while valence band is at least

energy level and partially loaded with electrons. The unfilled space between these two groups is called "band gap or forbidden band" and assumes a major part in the conductivity capacity of materials. In Figure2.3, electronic energy level for conductor, semiconductor, and insulators are overlapping. In conductors/metals, the conduction band and valence band are covered. Therefore, at a little connected electric field (little-biased voltage) electrons from the valence band effectively bounce to the conduction band (metals are great conductors of electricity). The band hole in a semiconductor is bigger than that of conductor and smaller than the insulator's band gap, along these lines, the more connected electric field is required to move electrons from the valence band to the conduction band in semiconductors than in conductors. Dielectric, then again, has an immense band hole contrasted with the other two. In this manner, the electrons can't do that and require a great deal more energy to hop the vacant space between the valence band and the conduction band, at that point dielectric can't permit flow of electric current (bad conductor of electricity).

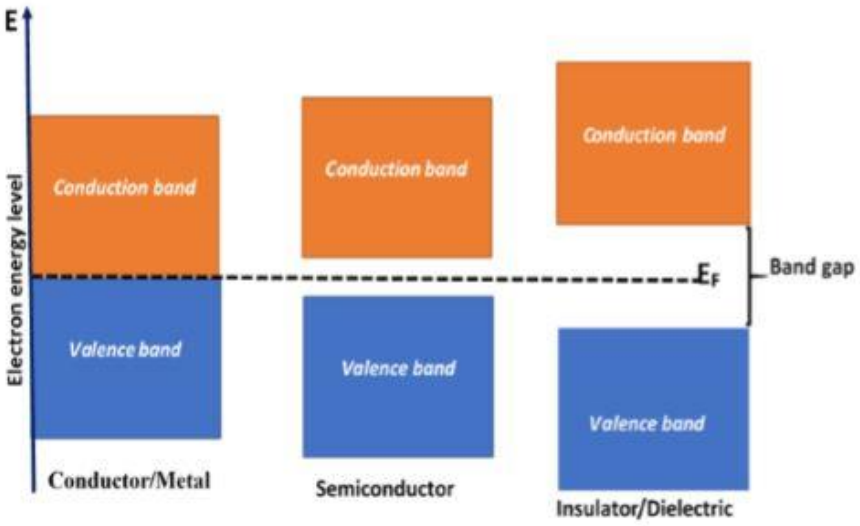

Figure 2.3. Energy band gap diagram for insulators, semiconductors and conductors. Dashed line represents the Fermi energy level [2].

It is not sufficiently beneficial to arrange materials on the basis of their electronic energy group levels. Few substances carry on like metal substances when seen electronically while optically go about as dielectrics. Indium tin oxide (ITO) is one case of those compounds which electronically responds as a metal substance (remarkable electrical conductivity), while optically carries on like a dielectric material (with magnificent optical transparency) and these properties make ITO to be generally utilized as a part of transparent electrodes in the picture and lighting domain. A few metals additionally show such behaviour, similar to tungsten/wolfram (W) which is actually a metal and is utilized to direct current in the light

bulbs, yet it acts like the lossy dielectric material in the visible spectrum range with a positive dielectric constant. Because of their little band gap, semiconductor materials, mostly utilized as a part of metamaterials outlines in the place of dielectric materıals. They are easily used to manipulate the propagation path of electromagnetic waves, where it can behave as a loss-free substrate or a lossy/absorbent layer depending on the range of the wavelength of interest. MMSs have been widely reported for practical EM applications due to their various advantageous features like:

1. MMSs plays a major and vital role in order to provide a multiband/ wideband frequency response.
2. MMSs are very helpful to achieve smart frequency response (i.e., simultaneous achievement of transmission and reflection characteristics), especially for the development of active EM structures.
3. Quite good microwave absorption properties can be obtained through MMSs.
4. The existing thickness-bandwidth tradeoff can be eliminated by the usage of such advanced EM structures.

However, MMSs are suffering from few limitations like complex optimization and fabrication steps. But the use of advanced EM software can simplify the task. Moreover, analytical techniques can be employed to solve the issues. The fabrication complexity is still a major challenge in front of the researchers, and work is still going on in this direction. Veselago's hypothesis about a negative permeability, permittivity prompts us to question ifparameters such as L' and C' in a system could likewise is created negative. Actually, from an impedance point of view, forcing a negative L' and C', or equally a negative shunt permission −jωC' and series impedance −jωL', basically exchange their susceptive and reactive parts, so that the series inductor turns into a series capacitor, and the shunt capacitor turns into a shunt inductor. The unit cell of the developing double structure appears in Fig. 2.4 (a), and it is effectively perceived as having the topology of a 2D high-pass filter organize. The effective permeability and permittivity represented by this topology can be appeared to be [12]:

$$\mu(\omega) = -\frac{1}{\omega^2 C' g} \tag{2.5}$$

$$\varepsilon(\omega) = -\frac{g}{\omega^2 L'} \tag{2.6}$$

where the disseminated parameters L' = Ld and C' = Cd are defined in the curious units [H·m] and [F·m], individually. Their importance is instinctively evident when the parameters are rather spoken to as 1/L' = (1/L)/d and 1/C' = (1/C)/d [12]. In spite of the outcomes for the RH

unit cell, the double system effective material parameters 7j are conspicuously negative. In any case, they express the functions of frequency and remain no longer constants; in spite of the fact that as far as possible is an idealized estimation. The specific dispersive structures guarantee that the time-averaged stored magnetic and electric energies related with this system are positive, so that the preservation of energy is not damaged. Therefore, the basic double high-pass arranges, with shunt inductance L' = Ld (H·m) and series arrangement capacitance C' = Cd (F·m) and, satisfies the vital prerequisite for LH behaviour; the effective material parameters are all the while negative. It was found the propagation constant helps in boosting the inverse relationship with frequency through the applications of the dual structure.

$$\beta = -\sqrt{-Z'Y'} = \frac{1}{\omega\sqrt{L'C'}} \tag{2.7}$$

corresponding ω–β curve is shown in Fig. 2.4 (b). For this case, there is antiparallel relation between group and phase velocities and are given by:

$$\upsilon\varphi = \frac{\omega}{\beta} = -\omega^2\sqrt{L'C'} = -\upsilon_g \tag{2.8}$$

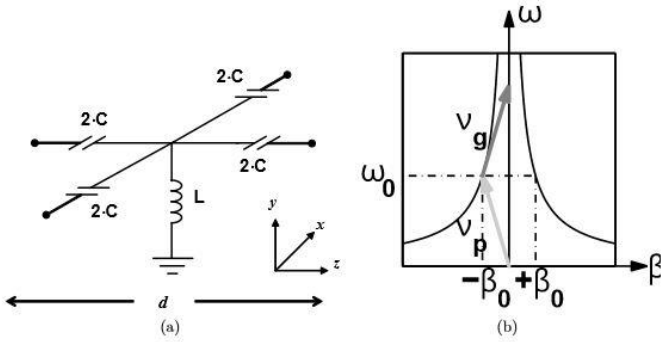

Figure2.4 a) Unit cell of 2D dual transmission line, and b) dispersion relation in a particular direction, i.e. x-z plane for the propagation having simultaneous negative parameters [7].

The relationship between the network characteristic impedance and effective wave impedance is also maintained:

$$n = \frac{c}{\upsilon\varphi} = \frac{\sqrt{\mu(\omega)\varepsilon(\omega)}}{\sqrt{\mu_0\varepsilon_0}} \tag{2.9}$$

$$n = \sqrt{\frac{\mu(\omega)}{\varepsilon(\omega)}} \tag{2.10}$$

The connection of a material and electromagnetic wave (light) is influenced gigantically by the electromagnetic properties like; electric magnetic permeability and permittivity. Normally, electric permittivity and magnetic permeability assume a vital part in the spread of

electromagnetic waves in a medium. This is because of the way that they are just parameters which are available for the dispersion condition. The electric permittivity characterizes the cooperation between the electric field and the reached medium while magnetic permeability decides how the material responds to an applied magnetic field and this can be portrayed by the accompanying dispersion relations:

$$k^2 = \varepsilon\mu\omega^2 \tag{2.11}$$

where ω and k depict wave number of theelectromagnetic wave, individually. The connection between angular frequency, a record of refraction (n) and wave vectors can be changed and becomes as follows[8]:

$$n = \sqrt{\mu\varepsilon} \tag{2.12}$$

$$\frac{k}{w} = n \tag{2.13}$$

It's undeniable from the above relations, that changing indication of ε and μ has no effect on these conditions. Vaselago clarified these by saying that if changing the indications of ε and μ has no effect, the materials with both negative ε and μ may not exist or regardless of the possibility that they exist, they should have properties not quite the same as those of natural materials. To clarify this he outlined two ideas. The idea of "Left handed materials" which are the materials or the medium in which monochromatic waves stream in unconventional way method for wave propagation resulting because of all negative signs of ε and μ in that medium. In such medium, the energy flux and the wave vector (Poynting vector) go in an inverse direction.

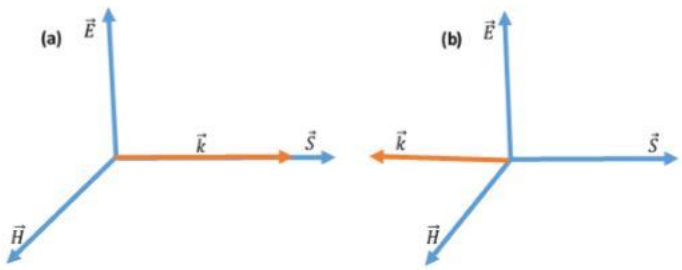

Figure 2.5. Geometric representation of $\vec{k}, \vec{H}, \vec{S}, \vec{E}$in: (a) Right handed materials and (b) Left handed materials [7].

In light of the above condition in electrodynamics, Poynting vector $\vec{S}$ and the fields $\vec{H}$ and $\vec{E}$ need to obey the correct hand rule and energy must stream in a similar direction with wave vector $\vec{k}$. Then again; in left handed materials, the two vectors $\vec{k}$and $\vec{S}$propogates in the inverse

direction. In this way, since vector $\vec{k}$ demonstrates the direction of phase velocity; in the left handed substances energy, streams the reverse direction to that of phase velocity. In other word left handed materials are called "negative group velocity materials".

2.1.3 CHIRAL MEDIA

The term chiral portrays an object, particularly a particle, which has or creates a non-superimposable identical representation of itself. This property changes the polarization of an electromagnetic wave (incident). In regular materials, chirality is normally weak and just at some exceptional frequencies. However, large chirality can be outlined with metamaterials at subjective frequencies. This property can be utilized as a part of polarizers, captivated channels, and energized splitters. Chiral media (CM) can turn the plane of polarization of the incident wave to one side or left relying upon the handedness of the items. This brings distinctive resonances for various circularly polarized (CP) incident waves. With respect to their interesting qualities, e.g., asymmetric circularly dichroism, transmission and optical movement, CMs have a lot of uses in the microwave and optical devices. A single layer metallic structure can likewise support chirality when the electromagnetic wave is incident diagonally. Another application of CM is chiral metamaterials (CMMs), that can demonstrate a negative refractive index (NRI) band, without the need both permeability and permittivity negative at the same time, as on account of customary NRI metamaterials (MMs).

2.2 DIFFERENT TYPES OF MMSs

2.2.1 TRADITIONAL CG BASED MMS

The operation system of traditional CGs depends on the resonating elements. Simply, the contemplation is that a plane-wave that illuminates a variety of metallic parts along these lines stimulating electric current on the segments. The amplitude of the produced current relies on upon the coupling of energy between the wave and the components. This coupling achieve huge amount of the fundamental frequency where the length of the components is a $\lambda/2$. Therefore, the components are formed with the goal that they are resonant near the frequency of operation. Contingent upon the dissemination, the current it goes about as an EM source, therefore creating a field i.e. scattered field. The scattered field added to the episode field constitutes the total field in the space incorporating the CG. By controlling the scattered field (arranging segments), in this way, the required filter response is made which can be found in the regime of the total field. As determined over, the appointment of the current on the parts chooses the frequency behaviour of the CG. The current itself depends on upon the shape of

the parts. Given the dependence of the conventional CG on the length, excitation of the higher-order modes, despite the first crucial mode, ends up detectably inevitable. Likewise, the frequency reaction of the conventional CG as a general rule has a high harmonic content. The first and the second possible modes show up in Fig. 2.6.

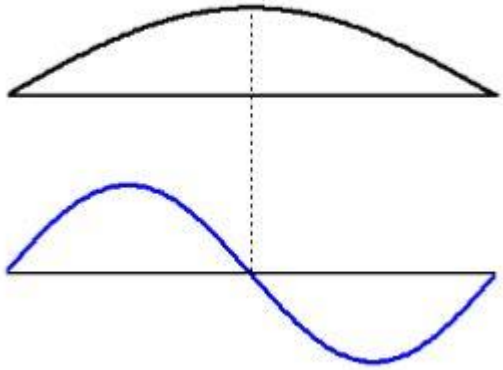

Figure2.6. The first and the second resonant modes- (top) shows the fundamental mode (frequency f) which is excited for any element shape irrespective os the incidence angle. (bottom) shows the first odd mode at about 2f which may be excited only at oblique incidence. The frequency of this mode may change slightly depending on the element shape [7].

The harmonic issues not only affects the CG frequency properties, additionally corrupts its output execution since a portion of the harmonics might be energized. These are energized due to the changes in the incident angle from ordinary to the CG plane. In spite of the fact that the geometry of the components has a basic influence on the filtering behavior, there are different parameters that can affect the frequency response. This could be the decision of the parameters of the substrate supporting the components of the CG and furthermore it's interelement spacing. The substrate appears to affects not only the operation of frequency but also the bandwidth of the reaction. The dispersing amongst the components, then again, calls attention to the problem of the grating lobe, the bigger the separating, the prior the onset of the grating lobes. Accordingly, a smaller between components is normally favoured. However, the dividing can likewise change the bandwidth; a bigger spacing delivers a smaller absorption bandwidth. To build up a superior comprehension of the operation of CG structures, a relative review over different sorts of CG is given here. In any case, first, we have in some way or another arranged CG structures. There are various imperatives in view of which CGs are categories. Here, we utilize Munk's approach which depends on the shape of components and are useful in characterizing CGs Figure 2.7 depicts the four main classes of CG geometries, demonstrated which are:

I) N-Poles or centre connected types, which includes the square spiral, Jerusalem cross, three legged element and dipole.
II) Types of loops such as the circular, hexagonal, square loops and four and three legged loaded elements, the circular loops, and the square and hexagonal loops.
III) Plate or Solid interiors plate types.
IV) Combination types

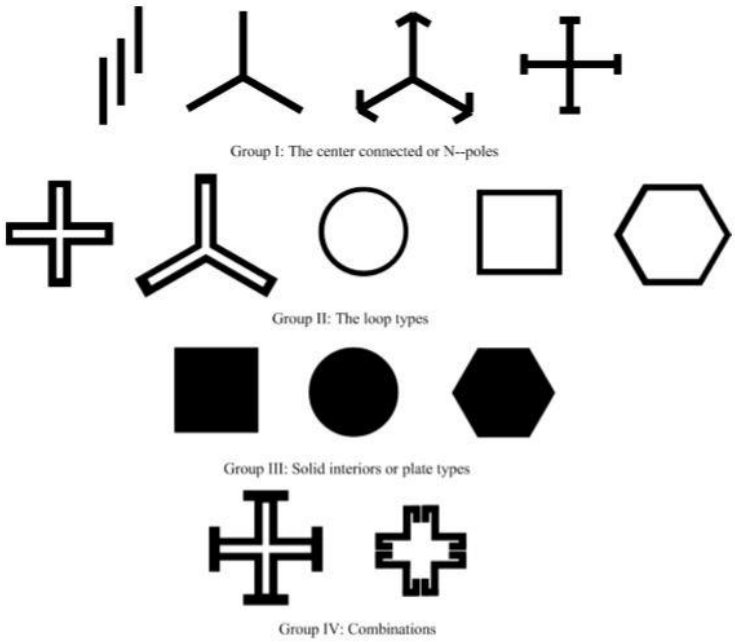

Figure 2.7. Four main groups of CG elements based on their shapes [8].

It was Veselago's charming guarantee of negative index materials at optical frequencies that has driven a significant measure of work in the metamaterial field. Throughout the most recent decade the principle drive in metamaterials research was to push the resonance of artificial materials to increasingly elevated frequencies with a definitive objective of making materials in the noticeable bit of the range. It was a fortuitous situation that this drive was reflected by significant progresses in nanofabrication instruments. These devices made it conceivable to configuration as well as to make and test structures with resonating properties from the microwave through the close IR. In 2007, Soukoulis et al. distributed an article depicting how the resonating results of metamaterials had been pushed from microwave [2]. The unit cell was on the request of millimeters. The drive to obvious wavelengths, be that as it may, uncovered the size impediment of the first split ring resonator design. This restriction has been an aftereffect of the way that metals don't work as perfect conductors in the noticeable range.

Wilbert et al. [12] researched the polarization insensitive MMSs through finite component numerical technique and another equivalent circuit electric model was proposed to translate

this polarization insensitivity. The models were fabricated to approve the model and exploratory values were appeared to be in great concurrence with the simulated results. Coordinating amongst both experimental and fabricated the resonance frequency and quality required considering a lower conductivity of the metal utilized as a part of the manufacture of the absorbing structure. These devices could be helpful for future frequency-selective detection applications.

Costa et al. [13] studied the well-known absorbing structure, referred to as perfect absorbing structures, containing metallic periodic pattern over a thin low-loss grounded substrate depending on an efficient transmission line display. This approach permits the inference of straightforward and simple closed formulas depicting the absorption component of the sub wavelength structure. The analytical type of the real piece of the input impedance was unequivocally determined to keep in mind the end goal to clarify why direct losses of the substrate are sufficient to accomplish coordinating with free space. The impact of the constituent parameters for tuning the working frequency and varying the absorption bandwidth was addressed. Finally, the angular stability of the absorbing structure has been examined.

Zhang et al. [14] introduced a design technique for broadband MMSs consolidating together the components of conducting geometries (CGs), magnetic absorbing sheet and sub wavelength opening arrays. The MMS has been developed of square leading patches periodic array installed into an attractive absorbing substrate backed by metal ground and punctured with circular hole array. The characteristics of magnetic absorbing substrate are enhanced and tuned by methods for puncturing holes and installing CGs. In order to enhance the measurements of the holes and CGs, the MMS with a thickness of 2.4 mm accomplishes a reflection coefficient under −10 dB from 6.3 to 17.3 GHz, which was almost 3.6 times the data transmission of the magnetic absorbing substrate. The deliberate outcomes additionally showed that the strategy for puncturing sub wavelength openings and implanting conductive CGs in the attractive sheet was practical to build the operation bandwidth of attractive sort RAs.

Ghosh et al. [15] demonstrates a straightforward design for making ultra-wide band ultrathin MMSs have been exhibited in microwave frequency range. The proposed structure was made out of two concentric circular split rings engraved on a metal-upheld dielectric substrate. A 10-dB absorption bandwidth from 7.8 to 12.2 GHz covering the entire X-band has been seen in numerical simulations under ordinary frequency. The composed MMS was minimal, ultrathin (only thick relating to focus frequency). In this way, the proposed structure was a decent option of other wideband MMS and can be utilized for some applications, for example,

electromagnetic interference (EMI), phase imaging, stealth innovation and electromagnetic compatibility (EMC).

Ghosh et al. [16] presented a proportional circuit model of an ultra-thin metamaterial absorbing structure including a square-ring-formed conducting geometry (CG). The model can be considered as arrangement resonators associated with short circuited transmission line and in parallel with coupling capacitance. The even and odd mode couplings have been joined to precisely decide the lumped parameters and additionally the absorption frequency of the absorbing structure. The impacts of substrate thickness and dielectric permittivity minor variation from the lumped parameters and full width at half- maximum (FWHM) bandwidth are explored in light of the proposed model. The proposed proportional circuit can be considered as a summed up model for analysed MMSs of subjective molded conducting geometries.

Lee et al. [17] worked on an ultra-thin CG MMS, comprising of a metallic ground plate and a CG, isolated by a solitary dielectric substrate, is presented. The above-mentioned MMSs have three extraordinary elements. They can have different absorbing bandwidth by altering the two absorbing peaks and, because of the high loss of the between advanced capacitor designs on the CG, the thickness of the MMS can be diminished to $0.04\lambda_g$. Also, the proposed MMS is insensitive to any polarized EM waves, attributable to the symmetric structure of the CG. In spite of the fact that we proposed a double band MMSs with two resonance response, one which controls multiple resonances reactions can be utilized to plan a more extensive bandwidth absorbing structure.

Panwar et al. [18] targeted to accomplish great absorption with wide bandwidth relates to reflection loss (RL) $\leq$ - 10 dB for lower thickness ($\leq$ 2.0 mm) by creating ferrite-graphene (FG) composites. A basic review has been done by differing the structure of FG to get wideband absorption with lower thickness. The compelling complex dielectric permittivity (ε', ε'') and effective magnetic permeability (μ', μ'') of composites were measured utilizing transmission/reflection waveguide strategy in the scope of 8.2 to 12.4 GHz. These measured ε', ε'', μ', and μ'' values have been utilized for the plan of single and double layer MMSs. The increasing G content in FG composites brought about a diminishment of thickness and wide absorption bandwidth. Further, multilayer approach was received to improve the radar wave absorption with broad bandwidth at a lower absorption layer thickness. The double layer MMSs demonstrates a solid RL of - 55.3 dB at 10.2 GHz with wide transmission capacity of 3.1 GHz in the frequency scope of 8.6 to 11.7 GHz. The multi-layering approach encouraged to

accomplish a lower absorption layer thickness of 1.7 mm. Discoveries give a successful and attainable approach to develop broadband and thin MMSs which might be used for stealth applications.

Ghosh et al. [19] introduced a switchable MMSs/reflector in light of active frequency selective surface (AFSS) has been introduced for broadband applications. The curiosity of the proposed configuration lies in its biasing system and symmetric configuration, which makes the structure polarization insensitive not at all like the prior revealed AFSSs. A solitary band switchable reflector/MMSs have at first been acknowledged, which has been portrayed through an equal circuit model to determine the circuit parameters. Afterward, surface-mount resistors have been actualized in the plan to understand a wideband switchable reflector/MMSs gone for C-band applications. The proposed structures have the benefits of angular stability, in addition single-band, simplified geometry, and wideband attributes contrasted with already revealed switchable reflectors/MMSs.

Unaldi et al. [20] displayed a review on novel ultra-thin double band conducting geometry (CG) for X band applications. The proposed single layer CG works as a band reject channel at 8.5 GHz and 10.5 GHz. The proportion of these two working groups has little values. Also, the outlined dual band single-layer CG has an ultra-thin thickness of **$0.021*\lambda_l$,** where λ_l was the wavelength of the lower operational frequency. The planned structure has double band reject channel trademark which gives a stable transmission execution at slant incident angle. Considering these properties as giving two firmly spaced resonating frequencies, the composed CG can be utilized as a part of double frequency applications at X band.

Panwar et al. [21] presents a review of recent improvements in the field of conducting geometries (CG) - based progressed electromagnetic (EM) structures. This paper manages a review of various CG geometries, to be active, nature inspired, traditional, multi-layered CG and three-dimensional and multi-layered CGs. Various CG structures having EM applications are discussed like microwave MMSs, antennas, textiles and radomes. In advance, extraordinary sorts of enhancement and creation procedures for CG-based EM structures are joined. It was clear from the survey that CG-based structures can be utilized for different applications over a wide frequency regime, including millimeter, microwave and terahertz waves. Sooner rather than later, some other novel uses of CGs are normal that can open another new door for researchers.

Li et al. [22] proposed a consolidated element technique which can be connected in planning double band MMSs. A double band MMSs were exhibited by presenting two components in

one unit cell. They first give two absorptive peaks which are confirmed by analyses. Two absorption crests show up close to 9.1 GHz and 11.8 GHz with an amount of 99.3% and 99.4%, separately. Second, field and current distribution was provided to better comprehend the physical component of the absorption. Finally, they researched the impacts of the dielectric-spacer thickness on the absorption. It was discovered that the thickness of the dielectric spacer provides sensitive effects on the magnetic absorption.

2.2.2 MULTIPOLE CG BASED MMS

This section displays a novel multiple miniaturized component CG having a low thickness and the desiredmultipole frequency reaction. For this plan, new miniaturized CG components are produced to accomplish a low thickness arrangement and enhanced functionality. The proposed CG empowers execution of higher order spatial filters over low-profile conformal antenna array. In the first place, the outline of a thin, modified miniaturized e CG delivering a single pole bandpass reaction and a transmission zero is introduced. The modified configuration is a single sided circuitboard with a specific unit cell comprising a loop focused on a wireframework. Next, utilizing a comparative metallic example on the opposite side of a substrate, a double band pass frequency response is delivered. This response is accomplished by picking proper dimensions of the loop and wire of each layer and by properly situating the layers regarding each other. To build up a benchmark, dualpole CGs utilizing cascaded layers of a formerly outlined miniaturized component CG are considered. In examination with the benchmark, the modified dualbandpass configuration has just two metallic layers, rather than four, and a single substrate, rather than three. The proposed multipole CG is λ/240 thick, which is six times thinner than the benchmark structures. Also, the frequency reaction of the new CG demonstrates higher out-of-band rejection esteems. Execution of the multipole screens is tried by manufacturing CGs with maximally-flat and double band pass reactions and measuring their frequency reactions.

2.2.3 RECONFIGURABLE MMSs

A reconfigurable miniaturized element, conducting geometry is displayed here. A standard waveguide estimation setup is utilized to assess the execution of the outline. The proposed CG comprises of two periodic arrays of the metallic loop, with a similar periodicity, on either side of a thin dielectric substrate. The tuning of the reconfigurable surface is demonstrated numerically to be conceivable by fusing tuning varactors into the structure. Utilizing varactors on both layers, a reconfigurable frequency response is accomplished, which has two methods

of operation: band stop and band pass. Additionally, two totally different methods of operation, the centre frequency, and also the bandwidth of the reaction can be tuned autonomously. Frequency tunability with a consistent bandwidth more than 3–3.5 GHz appears. A bandwidth tuning at a fixed centre frequency is additionally illustrated. The results are verified tentatively by creating models of the design at S-band loaded with lumped capacitors. To exhibit the tunability, different sets of fixed-values capacitors, instead of varactors, are utilized as a part of a waveguide estimation setup to maintain a strategic distance from difficulties related with biasing varactors in the waveguide. A reconfigurable miniaturized element CG is displayed in this part in which not just the bandwidth and the centre frequency can be independently tuned, additionally the reaction can be changed from band pass to stop the band. This CG has two varieties of loops imprinted on either side of a thin flexible substrate. The tunability of the outline can be accomplished by interfacing the loops on each layer by varactors.

2.2.4 RESISTOR BASED MMS

The wide bandwidth and good absorption characteristics are major requirements for a good MMS. MMSs loaded with chip resistors are known as resistor based MMSs. Resistor plays a major role in enhancing the properties of the different MMS. These splits created in the CG are used for inserting different lumped element. In general, the lumped elements incorporated could be resistors, capacitors or inductors. Figure 2.8 sketches the schematics of chip resistors, light dependent resistors, wire wound resistors, leaded resistors, surface mount resistors, etc., which can be utilized for aforementioned applications. Due to the losses present in the chip resistors, they can improve the bandwidth and absorption characteristics.

Figure 2.8. Distinct classes of resistors utilized
for various applications [8].

Metamaterial structures have wide applications in different areas, for example, wireless communication, stealth technology, radar cross section reduction and so forth. Conventional safeguards, for example, Salisbury screen, Jaumann absorbing structure utilize resistive sheets placed before a conducing plane to give absorption at certain resonant frequencies. In spite of the fact that they are straightforward in nature, their bandwidth are exceptionally narrow because of coordinating of quarter wavelength conditions at center frequencies. A few outlines, for example, lossy resistive, multi-layer structures, various resonances, sheet, and lumped resistors have been accounted to improve the bandwidth of electromagnetic (EM) wave safeguards. Among them, the circuit analog MMs was an effective solution for this narrow bandwidth issue, where the chip resistors are to be soldered on a metal patch imprinted on a grounded dielectric substrate. A few different geometries like consistent octagon, trumpet-formed, Jerusalem cross structures stacked with lumped resistors have additionally been introduced in before research.

Li et al. [23] researched incorporating of the lumped resistances into the twofold octagonal rings metamaterials, a thin, polarization-insensitive and wide MMSs experimentally and hypothetically. The ideal MMSs have been developed of twofold octagonal rings stacking the eight lumped resistances and the substrate with height of 3mm. The impacts of the twofold octagonal rings and eight lumped resistances are investigated by absorption and the electric field appropriations. The results show that the structure obtains absorption from 7.9 to 17.1GHz with absorptivity bigger than 90% at the incident points from 0^0 to 20^0 and accomplishes over wide absorption from 5.8 to 18GHz with a full width at half maximum at wide incident angles from 0^0 to 70^0.

Luo et al. [24] introduced another sort of Salisbury screen MMSs with a few symmetric fixed resistors in based on first order Minkowski loop NI surface. Results demonstrate that the aggregate thickness has been reduced significantly contrasted with traditional Salisbury screen. Absorbing impact and resonating frequency was affected by the estimation of resistors. As a result of the symmetry of structure the screen was not delicate to the direction angel with vertical incident wave. The MMSs not just has the benefits of thickness, thin substrate, wideband absorption bandwidth, additionally can possibly accomplish better execution in joining absorbing bands and diminishing structure size.

Costa et al. [25] presented a high-impedance surfaces (HIS) involving lossy conducting geometries (CG) which are utilized to configure thin electromagnetic MMSs. The structure, in spite of its ordinary resonating behavior, was ready to play out a wide band absorption in a

diminished thickness. Losses in the conducting geometry are presented by printing the periodic pattern through resistive inks and thus avoiding the soldering of lumped resistors. The impact of the surface resistance of the CG and dielectric substrate qualities on the information impedance of the MMSs were discussed by methods of circuital model. It has been demonstrated that the ideal value of surface resistance was influenced both by substrate parameters (thickness and permittivity) and by CG component shape. The equal circuit model was then used to present the working standards of the narrowband and the wideband absorbing structure and to derive the most appropriate component for wide band absorption.

Taylor et al. [26] presented a topology for two-state exchanging of a ring based CG. Offering great execution regarding all polarizations influenced and great angular stability, the ring component has been a mainstream decision in conducting geometry (CG) plans. The two states offered by the surface enable it to be either reflective or transparent at the frequency range selected. A plan focused at the 2.4 GHz WLAN band, and expected for the control of the electromagnetic characteristics of structures, was acknowledged both by estimation and simulation, the consequences of which are introduced and assessed.

Li et al. [27] introduced the fabrication, analysis, design, and measurement of a tunable broadband and low- frequency radar MMSs connected in the frequency regime of 1 to12GHz. Numerical results show that MMSs based on resistor- loaded conducting geometry (CG) can be resistively tuned to give a wideband absorption of surpassing 10dB in the range of 1 to 12 GHz. Additionally, prevalent absorbing execution can be accomplished by presenting capacitance paralleled with resistance. Estimation comes about demonstrate that the radar MMSs, by method for configuration with active CG (ACG) controlled by p-i-n diodes, can be tuned to give a consistently factor reflectivity level of under 10dB from 2 to 11.3 GHz with fluctuated predisposition voltages.

Fan et al. [28] proposed non foster loads based on a novel active MMS. Viable circuit model was logically illustrated, considering the material losses for diagonally incidence plane waves with both transverse- magnetic (TM) polarizations and transverse-electric (TE). In view of the circuit demonstrate, astability properties are acquainted to give the outline standards for the non- foster components to accomplish a wide- angle and wideband metamaterial MMSs (MA). On the basis of the resonant tunneling diodes these active components are accomplished by a two-port non- foster circuit. With the end goal of verification, showing a high electromagnetic absorption rate for wide angel and wide band, a sample active metamaterial MMSs

configuration was displayed, angle incidence for both TE and TM polarizations at microwave frequencies, when contrasted with its passive partner.

Yang et al. [29] presented an outline of broadband and thin utilizing a two-dimensional (2-D) periodic cluster of twofold square circles imprinted on a dielectric substrate. Lumped resistors are embedded into the four sides of the circles to absorb the incident electromagnetic wave. Measured and simulated outcomes for the radar cross-area (RCS) of a finite 2-D cluster of twofold square circles are in great agreement and both demonstrate that the novel MMSs can decrease a directing plate's RCS incredibly over a wide frequency regime.

Ford et al. [30] exhibited the outlines for an enhanced pyramidal geometric move radar absorbing material joining conducting geometries stacked with either lumped or distributed resistance. It was appeared, through full-field reproduction, that for a given MMSs, the consideration of impedance loading can diminish the frequency at which a 240 dB reflectivity level has been achieved from 6 to 2 GHz. Variable tolerance and oblique incidence are likewise discussed. It has been demonstrated that the consolidation of a resistively loaded square loop CG in the base locale of a pyramidal MMSs can give a beneficial change in bandwidth when contrasted and either an indistinguishable yet unmodified MMSs or one loaded with a PEC CG.

2.2.5 NATURE INSPIRED MMSs

The use of nature inspired MMSs (NI-MMSs) helped the designers to meet the requirements of high-performance circuit design and compact size in present day radar frameworks and microwave correspondence applications. The wider bandwidth and smaller sizes are few common advantages of NI-MMSs. The utilization of NI-MMSs have essentially affected numerous zones of science and designing; one of which is antennas. Nowadays researchers are employing such advanced EM structures for the development of thin and broadband microwave absorbers because of its different advantages like self-similarity,multibandresonance, and space-filling, etc. There might be a possibility to find new physical phenomena initiated by the cooperation of fields with nature inspired geometry. The destructive interference between reflected waves from two interfaces enormously decreases the reflection and upgrades the absorption.

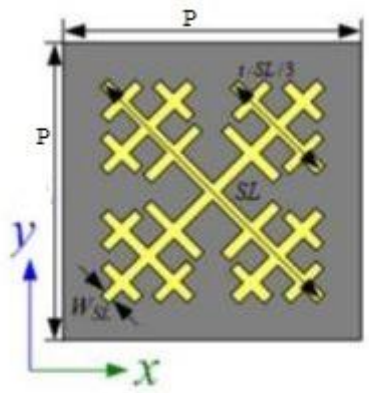

Figure 2.9. Cell element structure of CG with p as periodicity and W and SL as its dimensions [9].

In general, the radar wave absorption mechanism was assigned to complete impedance matching among dielectric and magnetic properties of materials. Therefore, MMSs can be engineered in such a way that the absorption properties of the MMS is dependent on its CG shape. In order to improve the absorption bandwidth issues nature inspired geometry based CG have been adopted. Nature inspired shapes possesses an interesting property, i.e. the self-similarity property. Briefly speaking, when there was the replication in the geometry of MMSs, self-similarity can be described. In self-similarity property the geometry of structure has been scaled at different levels within that same original structure. Thus, wideband and multiband behaviour were the results of the self-similarity of nature inspired structure. On the other hand, designing of the antenna and CG for their reduced sizes, nature inspired shapes can be used. In the previous years, various CG such as multipole, the multiband and band stop were successfully designed and fabricated using the nature inspired geometries.

Panwar et al. [11] presented the work with single and double layer coatings which exhibits a procedure of mixing the nature inspired geometry based conducting geometries (CG). These coatings are involved very much streamlined micrometer-sized (80–90 m) and Nano-sized (20–30 nm) Ti particles based Fe_3O_4 (80–100 nm) composites. The principle target of this review was to accomplish great absorption with wide bandwidth relating to RL ≤ 10 dB for less covering thickness (≤ 1.5mm). The nature inspired geometry based CGs have been planned to utilize an iterated work framework, which were inserted with single and twofold layer composite absorbing structure to analyse their impact on the MMSs. Therefore, on joining a Sierpinski gasket nature inspired CG with a double layer heterogeneous composite coatings turned out to be a decent idea that can be utilized for different practical applications.

Liao et al. [31] examined the impact of microwave absorbing material-based (MAM) substrate on the absorption properties of NI-CG MMSs in this paper. Various nature inspired shapes

were proposed so as to develop the schematic charts of the CG unit cell. The outcomes demonstrate that the strongest absorption performance (including bandwidth and peak value) has been accomplished with the expansion of the substrate thicknesses for the FR-4-based CG MMSs. Nonetheless, absorbing properties are significantly improved by utilizing similar thickness MAM-based substrate to supplant the FR-4 substrate. Therefore, a potential useful application are obtained from the method of presenting the MAM-based substrates rather than the traditional dielectric substrates in device miniaturization.

Panwar et al. [32] reviewed a basic examination has been done on more than three diverse sort of absorbing structures, i.e. Nature inspired CG sandwiched MMSs, double layer and NI-CG incorporated for accomplishing great absorption with bandwidth(RL $\leq$ 10 dB)and thickness (t $\leq$ 1.5 mm). The determination of appropriate composite, thickness and layer preferences has been improved utilizing genetic algorithm (GA) based on the magnetic permeability and effective complex dielectric permittivity of the integrated heterogeneous composites. The Sierpinski cover nature inspired CG sandwiched double layer MMSs (t = 1.3 mm) demonstrates a strongest RL of 41.2 dB at 8.7 GHz with wide bandwidth of 3.1 GHz in the scope of 8.2 to 11.3 GHz. The thin and broadband MMSs gives a feasible and effective answer for stealth application.

Zhao et al. [33] presented and fabricated a stop band conducting geometry (CG) with polarization strength and extraordinary incident angel. Every component of the CG comprises of four same second emphasis of H- shaped nature inspired parts and a cross spiral patch in revolution symmetry. For both TM and TE polarizations this CG shows extraordinary security with the occurrence angle going from 0° to 80°. Furthermore, fix measurement of the CG component can tune the resonant frequency. This implies the proposed CG can be connected has various potential values and are present in various frequency ranges and has potential value in handy applications.

2.3 APPLICATIONS OF MMSs

MMSs have extraordinary potential for the practical EM applications due to their numerous advantageous features as already discussed in the previous section. The brief overview of major applications is depicted below:

2.3.1 CLOAKS AND ABSORBERS

There are essentially three methods for decreasing electromagnetic dispersing as well as reflection by a protest; first is the absorption of the incident wave, second to cancel out the

magnetic and electric fields created by the object, and third to guide approaching waves around the object. The last two systems are alluded to as cloaking of the object.Cloaking of an object by directing the waves around it can be deciphered as changing the coordinate system. Cloaking can likewise be accomplished by the cancellation of the field created by the objective. This can be accomplished by utilizing cloak with magnetic and electrical polarizabilities equivalent and inverse to that of the objective. The other two strategies are, however, generally newer. Customarily radar absorbing structures have been utilized for reducing the reflections from the target surface in order to make the object invisible to the radar range. However, metamaterial absorbers are being explored, as one is not constrained to the electromagnetic qualities found in nature.

2.3.2 PHASE SHIFTERS

Among all the uncommon, yet downplayed, the scattering/dispersing properties are the principle purposes of interest for LH metamaterials. Without a doubt, the spread steady have opposite connection with the frequency, to such a degree, to the point that the effective wavelength portraying this fluctuations in respect to frequency. Subsequently, with metamaterials at lower frequencies. A specific electrical length can be proficient at low frequencies with metamaterials. Notwithstanding, there is another of result this declaration: at a given working frequency, scattered gadgets can be made physically small with metamaterials. One of the first employments of this thought was in the affirmation of metamaterial phase shifters including substituting segments of regular TLs and NRI-TL metamaterials. The general stage shift given by these structures essentially aggregates to the entire of the stage shifts contributed by the RH and LH constituent portions. In this way, these structures benefit from another supportive property of metamaterials: that the recognized stage movements can have negative values in the LH area, positive values in the RH region, and a zero value between these two regions. The zero-degree stage move is particularly important since this could somehow solitary be expert using a one-wavelength-long TL. Besides, it showed up in these works that the metamaterial stage shifters are more broadband than their RH delay-line accomplices. This is a result of the way that the frequency scattering of the LH region offsets that of the RH portions.

2.3.3 DIVIDERS/COUPLERS

Passive directional couplers and Power dividers are staples in the microwave and photonic circuit outlining since these devices from major building squares of various reasonable EM structures. Both sorts of gadgets are circled in that the control of their properties, including

power division, extent, bandwidth, coordinating, directivity, and isolation relies upon their electrical length, and subsequently, these structures can be physically broad at low frequencies. From the past discussion on metamaterial stage shifters, obviously metamaterials can be associated with the scaling down of couplers and dividers also. Metamaterial control dividers for antenna array (series fed) exhibited a 97% size diminishment appeared differently in relation to standard plans and the additional control over phase properties using NRI-TL metamaterials impelled the outline of novel moderate metamaterial baluns. TL-based metamaterial branch-line couplers furthermore demonstrated significant measure diminishes. In any case, metamaterials have moreover been associated with the plan of coupled-line couplers demonstrating fascinating phenomena and a great novel. For example, a coupled-line coupler containing a conventional microstrip line adjacent and NRI-TL metamaterial line produces contra-directional power flow when the lines are phase coordinated, an obvious contrast in the co-directional power flow expected of an additionally outlined microstrip-microstrip coupled-line coupler.

2.3.4 ANTENNAS

A part of the soonest and most fascinating employments of metamaterials thoughts were made with regards to antennas. Metamaterials can be used to change, improve, or generally propel the properties of gathering reception apparatuses by optimizing in different ways. For example, their novel dispersive and possibly low-loss properties can be reduced to either lessen bar squinting or empower frequency tuning. Their stage remuneration properties can be utilized to design the small antennas sustain apparatus and scaled down component themselves. Also, their natural ability to help fast (waves with a stage speed more conspicuous than the speed of light in vacuum) engages them to go about as a leaky wave antenna with phenomenal radiation properties. Regular gathering reception antennas have in like manner benefitted from metamaterials used as directing geometries or immaculate attractive conductors/artificial (PMC/AMC) composed into ground planes to overhaul radiation properties by suppressing surface-wave losses or wiping out the quarter-wavelength remove that disengages a receiving antenna and its PEC reflector. Regardless, these surfaces are generally classified as electromagnetic/photonic band hole (EBG/PBG) structures.

Radiation by a technique for leaky modes delineates a steady coupling from a rapid wave structure into free space. Certainly, the upper-frequency area of the LH or NRI pass band talks about a condition wherein the stage speed of the guided wave in the metamaterial surpasses that of free space, and power is leaked from the metamaterial. In any case, metamaterial leaky

wave receiving antenna differ from traditional receiving antennas in that stage coordinating of the guided backward wave mode and the broken forward-wave mode requests that the last ascents at backward (or negative) point. In a backward leaky wave, fan-pillar radiation was first showed up using a 1D CPS-based NRI-TL imperfect wave getting wire working at 15GHz. Besides, since the scattering characteristics of these metamaterials can be made to pass particularly.

The leaky waves from the LH (NRI) to RH (PRI), make a move as needs be, transmitting from negative to positive focuses through broadside. This was showed up in 1D using both passive and dynamic tunable TL-based defective wave accepting receiving antenna and for leaky wave pencil beams likewise, cone-like bars using an inactive 2D planar NRI-TL metamaterial surface. Several of these exploratory results are also maintained by basic theoretical surveys setting up the method for cracked wave radiation identified with various metamaterials.

Small reception antennas apparatuses have been a subject of advancing investigation in a general sense since it has been difficult to make such receiving antennas (because of both low radiation resistances and the failure to match such getting antennas to authentic sources originating from the broad measure of responsive power stored in the nearby field). Moreover, to be pragmatic there ought to be adequately improved bandwidth. The standard of phase compensation, which engages considerable electrical lengths over smaller physical lengths is, along these lines, of staggering criticalness to these efforts. Without a doubt, the loading of common accepting antennas using LH metamaterials bringing down their resonance frequencies. Compact metamaterial arrangement nourished getting receiving antennas similarly pushed the outline of little ring accepting reception apparatus in which segments are supported in stage using zero-degree NRI-TL metamaterial lines and composed in a ring of sub-wavelength estimations. The use of round metamaterial shells or even individual metamaterial-propelled open parts too resonantly cancels the effects of the close field have additionally been proposed, and indicate ensure in beating the organizing issue. Clearly, antennas supports frameworks can in like manner be scaled down by using decreased metamaterial stage shifters.

2.4 RESEARCH GAPS

- When we increase the bandwidth then thickness of the material is also increased but in our model we need to reduce the thickness so for that purpose FSS structures of different shapes are used to reduce the thickness along with the decrease in bandwidth.

- As there are large number of materials in library which can be used for structures, now its complex process to optimise the best three materials to have reduced thickness, reflection loss and increased bandwidth.
- There are large number of materials which can be used as model or as FSS structures in our models so it's very difficult to choose the optimised material for the model giving the best interface.
- It is difficult to fabricate such kind of complex structures.

CHAPTER 3

DESIGN OF RESISTOR LOADED SQUARE APERTURE GEOMETRIES

Nowadays there is a demand of thin and broadband MMSs that can provide better absorption performance. The requirement of broadband frequency response can be fulfilled by adapting advanced EM structures like conducting geometries (CG). CG are aperture /patch shaped periodic structures used for filtering operations, depending on frequency selective characteristics they may be high, low, band pass or band stop filters [6]. It is well known that the CG geometry, inter element spacing, type and substrate of CG are parameters that greatly affects the EM performance. A very good pioneer work has been reported by the researchers, but still there is a need to analyse the effect of patch/aperture CG geometries over the performance of MMSs. So, the effort has been made to achieve the main target of this paper i.e. to examine the effect of CG geometries (Patch/Aperture).The next aim of Further, bandwidth of MMS has been enhanced by incorporating lumped resistive circuit elements in the range of 2 to 18 GHz.

3.1 DESIGN OF DISTINCT MMSs

A. Patch and Aperture geometry based MMSs

It is well known that CG geometry greatly affects the frequency response of the EM structures, therefore, it is interesting to examine the effect of patch and aperture geometries over the absorption characteristics of MMSs [19, 20]. In this section, the numerical analysis of different MMSs has been carried out using advanced EM software i.e., CST Microwave Studio. The proposed MMS consists of an aperture/patch geometry impacted dielectric layer of FR4 material (with dielectric constant 4.3 and loss tangent tan δ=0.025) backed with a perfect electric conductor (PEC). The thickness values for dielectric and PEC layer is 3.0 mm and 2.0 mm, respectively. The absorption (A(ω)) from the structure can be found out, where S_{11} is reflection coefficient and S_{21} is transmission coefficient.

Based on a critical literature review, the circular, square and cross geometries have been chosen for the current study. Figure 3.1 (a)-(f) sketches the patch/aperture geometries and corresponding design variables for the MMSs, where grey region represents the conductive

surface of the copper (annealed). So, in this manner, the proposed EM structures can be categorized as follows:

- Category I: Patch geometries of circular, cross, and square as shown in the figure 3.1 (a)-(c).
- Category II: Aperture geometries of circular, crosses and square as shown in the figure 3.1 (d)-(f).

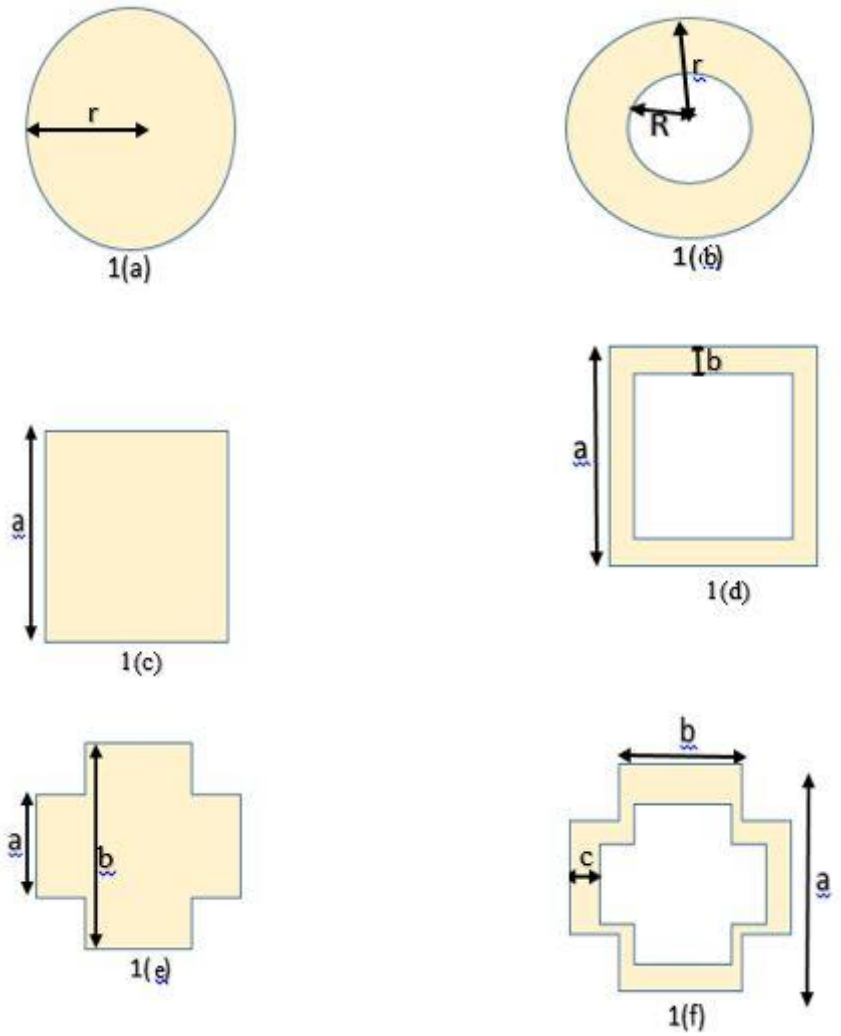

Figure 3.1: Patch and aperture CGs geometries utilized for the current study (a) Circular patch, (b) Square patch, (c) Cross patch, (d) Circular aperture, (e) Square aperture and (f) Cross aperture.

The Floquet theroem has been utilized in order to develop periodic EM structures and accordingly the unit cells with size 10 mm × 10 mm has been utilized. Boundary conditions are applied to the MMSs to determine the model scope, to truncate the infinite space to finitie volume and they can also help in reducing the transmission time and computation demands. In this paper periodic boundaries are applied to provide periodicity to the unit cell MMSs.

Parametric analysis had been performed to get the optimised results and parameters as shown in figure 3.4(a)-(c) and Table 3.1-3.3

TABLE 3.1.
DETAILS OF OPTIMAL DESIGN VARIABLES FOR PATCH APERTURE CIRCULAR GEOMETRIES.

Geometry	Design variable	Value
Patch	*r*	5.0 mm
Aperture	*r*	4.0 mm
	R	3.0 mm

TABLE 3.2.
DETAILS OF OPTIMAL DESIGN VARIABLES FOR PATCH APERTURE SQUARE GEOMETRIES

Geometry	Design variable	Value
Square patch	a	4.0 mm
Square aperture	a	1.0 mm
	b	8.0 mm

TABLE 3.3
DETAILS OF OPTIMAL DESIGN VARIABLES FOR PATCH APERTURE CROSS GEOMETRIES.

Geometries	Design variable	Value
Cross patch	a	2.0 mm
	b	6.0 mm
Cross aperture	a	4.0 mm
	b	2.0 mm
	c	0.5 mm

B. Lumped resistor element (LRE) based MMSs

The unit cell geometry of LRE-MMS with optimized dimensions is depicted in the Figure 3.2. The proposed design constitutes metallic patch imprinted dielectric substrate. The CG is in shape of a single square loop having splits at the centre of each arms of the square. The split positions in square loops are occupied by inserting the lumped resistors Rc [8]. FR4 with relative permittivity (ε_r) of 4.3 and loss tangent (tan δ) of 0.025 has been used as a dielectric substrate having thickness (T). The top CG is made of copper metal with conductivity of 5.8×10^7 S/m and thickness (k).

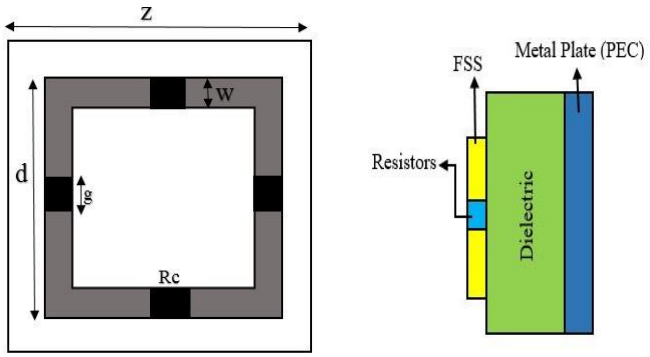

Figure 3.2: Unit cell geometry of the proposed absorber: (a) top view and (b) side view.

C. Spacer incorporated LRE based MMSs

Further in advancement, MMSs are then modified by including Spacer in between metallic patch and dielectric substrate. The CG shape is single, double and triple square loop having splits at center of each arms of the square. The split positions are occupied by inserting the lumped resistors R1, R2 and R3.[8] Rogers RT5880 (loss free) with relative permittivity (ε_r) of 2.25 and loss tangent (tan δ) of 0.001 has been used dielectric substrate having thickness (t). Spacer with relative permittivity (ε_r) of 1.05 and loss tangent (tan δ) of 0.0017 has been used in between the layers having thickness (h). The unit cell geometries with optimized dimensions are depicted in the Figure. 3.3.

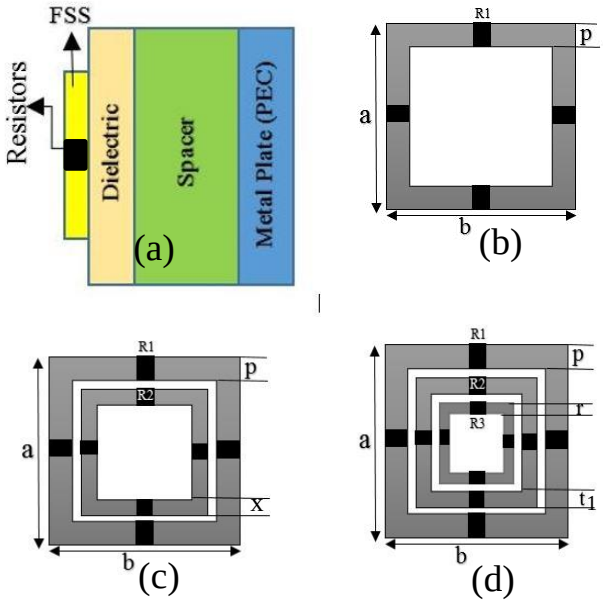

Figure 3.3: Unit cell geometry of the proposed absorber: (a) Side view and (b) - (d) top views of Single CG, Double CG and Triple CG.

The metamaterial structure is simulated in CST software using floquet ports with periodic boundary conditions which demonstrate that reflection coefficient over frequency range of 2to

18 GHz is less than -10 dB. Table 3.4 shows the optimized parameters and their values for MMSs.

TABLE 3.4

OPTIMIZED PARAMETERSAND VALUES

Parameters	Values	Parameters	Values
z	12.5 mm	r	0.5 mm
d	8.0 mm	x	1.25 mm
w	1.25 mm	t1	0.75 mm
Rc	100 Ω	R1	200 Ω
g	1.2 mm	R2	700 Ω
T	4.2 mm	R3	800 Ω
k	0.035 mm	h	3.8 mm
l	2.0 mm	b	10 mm
a	10 mm	p	1.25 mm

3.2 RESULTS AND DISCUSSIONS

a) Effect of patch/aperture geometries

Figure 3.4 (a)-(c) shows the frequency dependent RL characteristics of patch/aperture geometry based MMSs. Since the transmission of an incident wave is through the structure, completely backed by metal ground, the absorption can be calculated by the following equation:

$$A(\omega) = 1 - |S_{11}|^2 - |S_{21}|^2 = 1 - |S_{11}|^2$$

where S_{11} is reflection coefficient and S_{21} is transmission coefficient. When an EM wave is incident on any interface separating two media, the reflection and transmission are mainly governed by the media intrinsic impedances. If there is no transmission due to the complete metal backing, the absorption of the incident wave in the second medium can be maximized by minimizing the reflectivity only and that can be possible by proper admittance matching at the interface. After obtaining the results, it is observed that square patch achieve its peak RL value of -12.1 dB at the frequency at 16.5 GHz with the bandwidth of 0.2 GHz. On the other hand, when square aperture geometry is considered, it possess the resonating frequency at 17.3GHz

with the peak RL value of -6.7 dB. The overall performance of patch geometry is better as compared to other geometries as far as the requirement of wide absorption bandwidth is concerned.

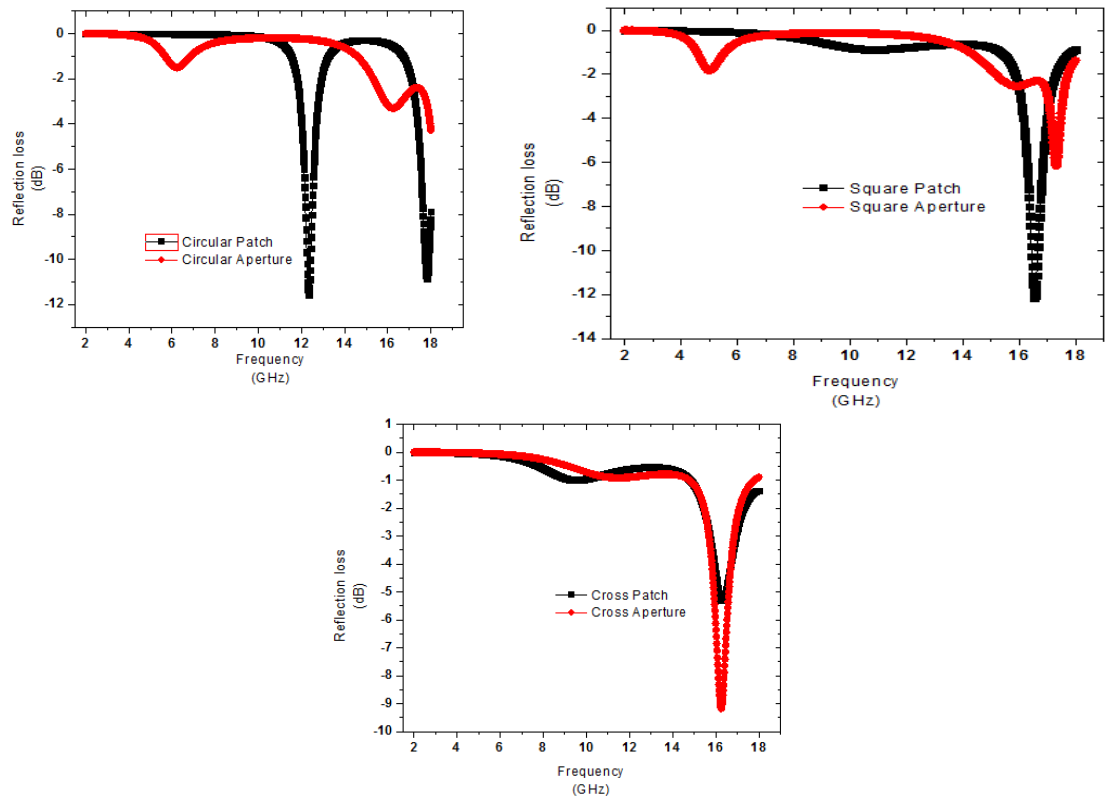

Figure 3.4. Frequency dependent characteristics for patch/aperture geometry based MMSs (a). Circular (b) square and (c) cross in the range of 2 to 18 GHz.

b) Effect of Resistor incorporation over RL characteristics.

In view of the above outcomes, it is clearly obvious that the outcomes are not according to the expectations as far as wide absorption bandwidth is concerned. Recently, it was investigated that incorporation of R expands the absorption bandwidth properties [37]. The loaded resistors can consume part of the EM energy and thus realizing the increased BW [40].Inspired by these researchers, the effect of inserting resistors over the RL characteristics of an optimal MMS is adopted. Figure3.5 (a) shows the RL characteristics of the MMS with and without resistors. In the other aspects, the absorption properties can be enhanced by improving the thickness of dielectric substrate (t) ranging from 1.0 to 5.0 mm. As the substrate thickness is diminished, a comparable decrease in the absorption values has been observed. The MMS with thickness (t) of 4.2 mm provides the best

outcomes with the bandwidth of 4.3 GHz and -48.5 dB peak RL value as depicted in the Figure 3.5 (b).

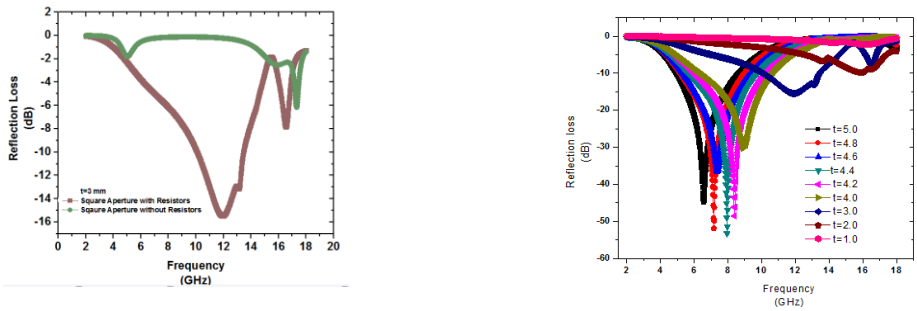

Figure 3.5. Frequency dependent characteristics for (a) Square Aperture geometry with and without Resistor incorporation and (b) Varying thickness of the dielectric substrate in the range of 2 to 18 GHz.

The performance of MMSs is greatly influenced by the resistance values [39]. So the next step is to examine the effect of resistance variation over RL characteristics of MMSs. In order to achieve the goal, the resistance value has been varied from 80 Ω to 180 Ω. The corresponding RL-frequency spectra's for varied resistance values are shown in the Figure.3.6. The MMSs with the resistance value of 100 Ω has been found to possess an optimal result. Figure 3.7 demonstrate that for ideal frequency response, R=100 Ω is embedded to give the best RL at 4.5 GHz with peak RL estimation of - 33.7 dB.

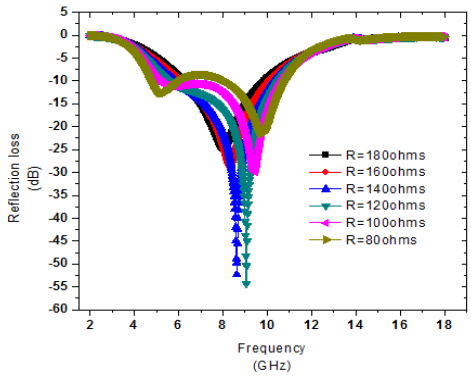

Figure 3.6. Frequency dependent RL values with varying resistance in the range of 2 to 18 GHz.

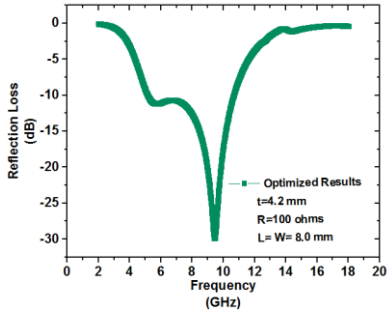

Figure 3.7. RL-frequency spectra for an optimal MMS (t=4.2 mm, R= 100, and L=W=8.0 mm) in the range of 2 to 18 GHz.

c) Effect of the spacer on RL characteristics

The absorption bandwidth corresponding to RL ≤ -10 dB is the foremost requirement to achieve the good absorption characteristics. The incorporation of the spacer layer can improve the bandwidth of MMSs [38]. Therefore an effort has been made to examine the effect of the spacer thickness over the RL characteristics. An intact structure is developed adding the spacer (ε'=1.05 and tan δ=0.0017) in between ground plane (PEC) and the dielectric substrate. The result shows that the reflectivity and resonance frequency can be changed on introducing the spacer in design as shown in Figure 3.8. Most importantly a tremendous enhancement has been observed in the -10 dB absorption bandwidth. The MMS structure with spacer layer of thickness 3.8 mm has been found to provide a -10 dB absorption bandwidth of 13.1 GHz in the range of 4.9 GHz and 18.0 GHz The peak RL value of -12.6 dB and it has been observed that there is a shift in the resonance the frequency higher to the lower frequency.

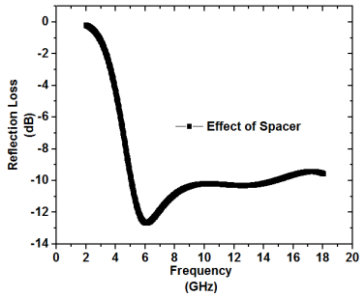

Figure 3.8. Frequency dependent characteristics showing the effect of spacer in MMSs.

d) Effect of aperture geometry variations over RL characteristics

The effect of aperture geometry variations has been demonstrated only for the optimal MMSs with spacer (as depicted in Figure.3.8). It is well known that the nature inspired geometry has higher electrical length, which reduces the absorption frequencies and makes the unit cell compact [42][43] Since the absorption peaks because of the individual split rings are well separated from each other, there is a minor change in absorption frequencies of the external ring when the inward ring is implanted inside [39].Therefore, it is possible to design a broadband MMS by varying the geometry of the proposed structure. Figure3.9 provides the correlation between simulations of various aperture geometries introduced. It is outlined that the absorption characteristics of Triple Square (TS)-MMS is better than Single Square (SS)-MMS and Double Square (DS)-MMS. A TS-MMS structure is found

to accomplish more extensive peak RL value of - 14.5 dB at 6.2 GHz with wide bandwidth of 13. 0 GHz (4.9- 18.0 GHz).

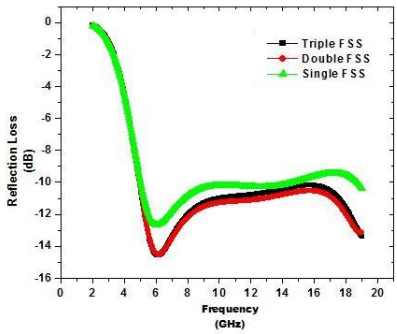

Figure 3.9. The absorbing performance of various aperture iterations.

e) Critical analysis of RL characteristics of TS- MMSs

The critical analysis of RL characteristics of developed TS-MMS structure has been carried out using the parametric analysis. In this section, three main aspects are primarily targeted such as (a). Effect of the resistance variation, (b). Effect of the dielectric constant value and (c) Effect of the substrate thickness and (d) Effect of the spacer layer thickness on RL characteristics. In order to examine the effect of the resistance insertion, three resistor R1, R2, R3 have been considered, where resistor R1 is embedded in the outermost loop, R2 in the intermediate loop and R3 is incorporated in the inner loop. From the studies, it is concluded that, the absorption characteristics can be controlled by changing the value of resistors. The lumped resistors absorb the electric currents [40]. They are located at areas with strong current so as to absorb power effectively. The graph of RL characteristics for variable resistance value of R1, R2 and R3 are depicted in Figures 3.10(a)-(c), respectively. From the detailed analysis, it has been clearly observed that, as the value of the resistance varies, the RL characteristics are greatly enhanced. Moreover, the absorption bandwidth is broadened to the great extent with bandwidth value of 13 GHz. Figure 3.10(a) shows the RL characteristics of TS- MMS where the resistance value of R1 is varied in the range of 100 to 500 Ω by keeping R2 and R3 as constant. As the value of R1 varies, it greatly influence the RL characteristics of TS- MMS. At R1 =200 Ω, the bandwidth of MMSs is noticeably increased with the value of 13.0 GHz. Furthermore, the value of R2 is varied from 500 to 800 Ω keeping R1 and R3 constant as shown in figure 3.10(b). The improved RL characteristics has been achieved at optimal resistance value of R2 =700 Ω with peak RL value of -14.5 dB at 6.2 GHz. Similarly in figure 3.10 (c), it has been seen that on varying the value of R3, there is change in the RL characteristics of TS-MMS. The improved results are obtained with R3= 800 Ω with bandwidth of 13.0 GHz ranging

from 4.9 to 18.0 GHz. Therefore, it can be concluded that enhanced RL characteristics and bandwidth are achieved due to the lossy characteristics of the resistors.

The dielectric constant significantly affects the reflection and transmission characteristics of MMS [21]. Therefore an effort has been made to examine the effect of dielectric constant on the RL characteristics of TS- MMS. The dielectric constant values have been varied from 2-13. The substrates with ε' =2.2 (Rogers), 5.9 (ferro), 10 (Arlon 1000) and 12.9 (Gallium Arsenide) have been chosen for the current study. The frequency dependent RL characteristics of TS- MMS with distinctive substrates are shown in the figure 3.11 (a). It is clearly observed that, resonant frequencies decreases with the corresponding increase in the dielectric constant values. The resonance frequency and bandwidth of the TS- MMS decrease with increasing dielectric substrate constant. This variation is mainly due to decreasing of the fringing fields and decreasing of the patch area [44]. Thus, the lower dielectric substrate permittivity gives higher value of electrical parameters of MMS. The MMS having dielectric constant (ε') value of 2.2 is found to provide broadband absorption characteristics as compared to the high dielectric constant substrate. The reason is that for very high values of permittivity there may be an impedance mismatch at dielectric- air interface.

The use of traditional absorbers was limited due to the certain thickness limitations. As per the quarter wavelength thickness effect, there is a direct relationship between wavelength and medium characteristics. The analyzed results of MMS for different values of substrate thickness (t) ranging from 0.8 to 3.2 mm is presented in figure 3.11(b). It is seen that when t increases, absorption results gets deteriorated. It is also noticed that minimal is the thickness, broader is the bandwidth of MMS. The observed results shows the peak RL value of -14.5 dB at 6.2 GHz with a wide bandwidth of13.0 GHz (4.9 to 18.0 GHz).From figure 3.11(c) it is clearly seen that when thickness increases from 1.8 mm to 3.8 mm, the resonating frequency changes accordingly and whole curve shifts towards the lower frequency end. It is clearly observed that the bandwidth has been increased to 13.0 GHz with RL value of -14.5 dB at 6.2 GHz.

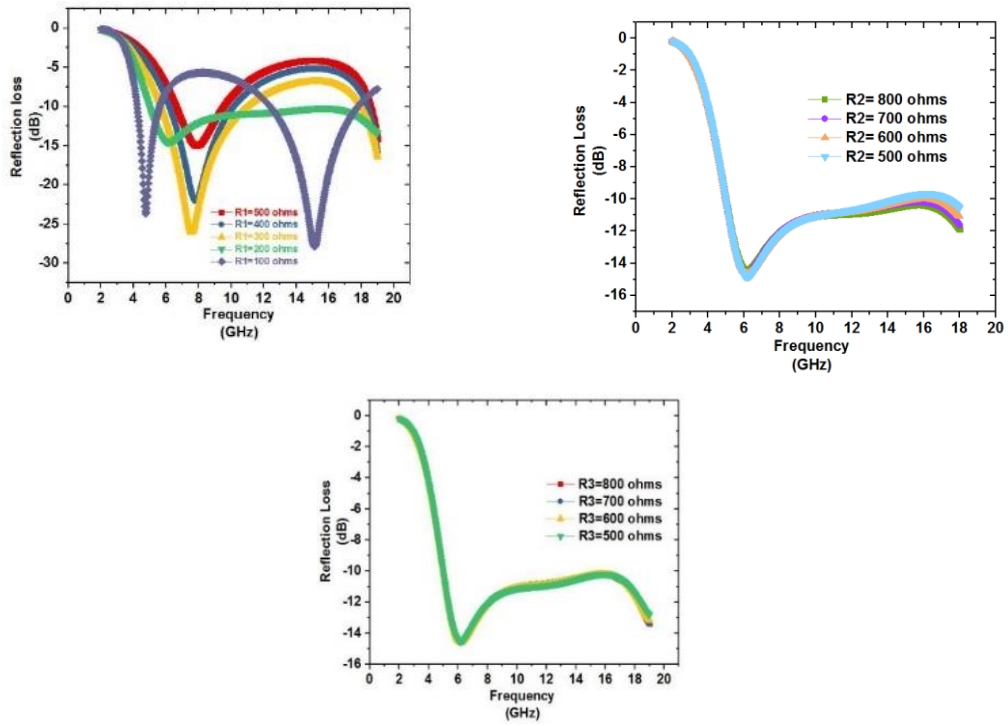

Figure 3.10. The measured reflection characteristics of (a) Resistance of outermost layer varies (R1), (b) Resistance of middle layer varies (R2) and (c) Resistance of deepest layer varies (R3) in the range of 2 to 18 GHz.

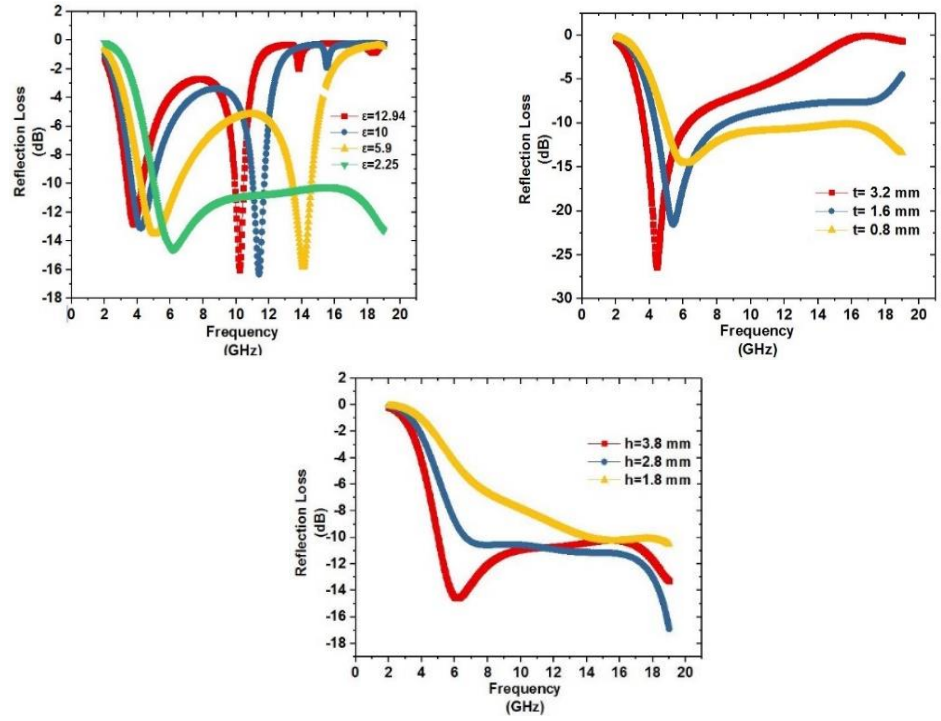

Figure 3.11. RL-frequency spectra for varying (a) Dielectric value (ε′) varies, (b) Dielectric thickness (t) varies and (c) Spacer thickness (h) varies in the range of 2 to 18 GHz.

3.3 CONCLUSION

This work guidelines for designing the broadband MMSs by the application of resistor loaded conducting geometries (CG). Various parameters are analysed to enhance the bandwidth of structure such as effect of the dielectric & spacer thickness, dielectric constant and the resistance values. The achieved reflection coefficient for the proposed MMS is less than -10 dB from 4.9 to 18.0 GHz. Unlike the previously reported research, this research is advantageous because the proposed MMS shows minimum reflectivity along with the wider bandwidth. This study will help the researchers to build more advanced EM structures in a more effective and concise way.

CHAPTER 4

DESIGN OF RESISTOR LOADED NATURE INSPIRED GEOMETRY

Nowadays there is a requirement of MMSs having good absorption characteristics along with the broader bandwidth. This requirement can be fulfilled by adapting EM structures like nature inspired CGs (NI-CGs).It is well known that the NI-CGs plays a significant role to provide a multiband frequency response, compactness and improved EM properties [45].The EM characteristics of NI-CGs depends on CG shape, CG iteration order and dielectric constant of the substrate. Moreover, an incorporation of chip resistors can further improve the reflectivity characteristics of NI-CG based MMSs. Therefore, an effort has been made to carry out a critical analysis of design parameters for the proposed MMSs.

4.1 THEORETICAL BACKGROUND

NI –CGs can be employed for the fulfilment of broadband absorption due to its attractive features like space-filling, multiband resonance, and self-similarity. There might be probability to find new physical phenomena incited by the interaction of fields with NI geometry. The destructive interference between reflected waves from two interfaces enormously decreases the reflection and improves the absorption. The wideband properties of NI- CG and loss properties of multilayer structure might be required to give great absorption. The attenuation of EM wave may create an electric field which collaborates with the portable electrons and initiates currents. The wave cooperation with NI-CG loaded MMSs bring about different inner reflections that give rise to a series of emerging waves, subsequently, microwave travels longer and more absorption happens. When an EM wave is incident on a metal backed MMS, the connection amongst absorptivity and reflectance can be composed as:

$$A(\omega) = 1 - |S_{11}(\omega)|^2 \quad (4.1)$$

where $|S_{11}(x)|^2$, A (x), are the reflectance and absorbance, respectively, at an angular frequency x. This reflection coefficient can be calculated as:

$$S_{11} = \frac{Y0 - Yin}{Y0 + Yin} \quad (4.2)$$

where Y_{in} and Y_0 are the input admittance of the structure and the admittance of air, respectively, which are presented in the equivalent circuit model of the structure designated as Figure 4.1.

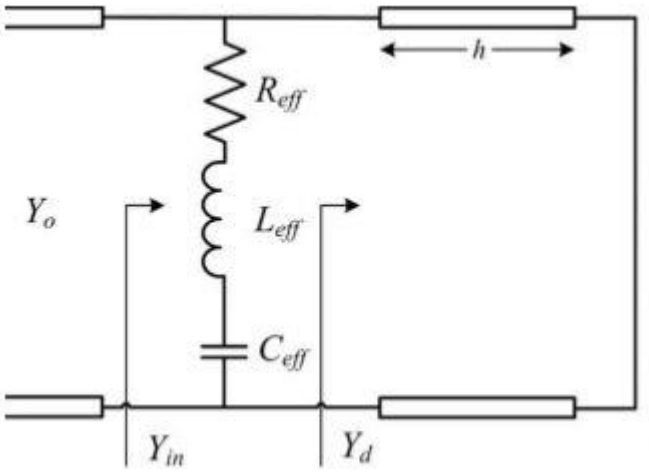

Figure 4.1. Equivalent circuit model [37]

This equivalent circuit of the proposed MMS comprises a metallic-based CG patterned on the top surface, which can be displayed as an RLC series circuit and a transmission line shaped by the dielectric substrate ended by metal ground plane. In this manner, the input admittance of the structure can be shown as follows [37]:

$$Y_{in} = Y_{CG} + Y_d \tag{4.3}$$

where

$$Y_{CG} = \frac{1}{R_{eff} + j\omega L_{eff} - \frac{j}{\omega C_{eff}}} = G + jB \tag{4.4}$$

$$G = \frac{\omega^2 R_{2eff} C_{2eff}}{\omega^2 R_{2eff} C_{2eff} + (1 - \omega^2 L_{eff} C_{2eff})2} \tag{4.5}$$

$$B = \frac{\omega C_{eff} (1 - \omega^2 L_{eff} C_{2eff})}{\omega^2 R_{2eff} C_{2eff} + (1 - \omega^2 L_{eff} C_{2eff})2} \tag{4.6}$$

$$Y_d = j\sqrt{\varepsilon_0 \varepsilon_r / \mu_0 \mu_r} cot(kh) \tag{4.7}$$

where μ_r and ε_r are the relative permeability and permittivity of the dielectric substrate, respectively, while k being the wave number of the incident EM wave in the dielectric medium which in turn can be written as $k = k\sqrt{\mu_r \varepsilon_r}$

At the point when an EM wave is incident on any interface isolating two media, the transmission and reflection of the wave are fundamentally represented by the intrinsic impedances of the two media [37]. If there is no transmission because of finish metal backing, the absorption of the incident wave in the second medium can be maximized by limiting the reflectivity just and that can be conceivable by proper admittance matching at the interface as seen from above equations. As the input admittance (Y_{in}) of the proposed structure is the parallel combination of the finished dielectric admittance (Y_d) and the top CG admittance (Y_{CG}), the susceptance of Y_{CG} must be counteracted by the susceptance of Y_d to make the general induction (Y_{in}) genuine and at exactly that point the input admittance will coordinate the free space admittance, therefore cause near unity absorption.

4.2 DESIGN OF NI-CG BASED MMS

The Minkowski loop based NI-CG has been modeled by constituting eight rectangular splits in each arm of conducting layer on the top metallic layer as presented in figures 4.2(a) and (b). The rectangular splits are designed to insert resistors with variable values. Figures 4.2 and 4.3 shows the side and top view of first and second order Minkowskiloop NI-CG based MMS. The proposed design is symmetrical in both x and y-axis. The numerical analysis of different MMSs has been carried out using advanced EM software, i.e., CST Microwave Studio in the frequency range of 2 to 18 GHz. The line width and resistance for the outer loop is W_{out} and R_{out} and same for the inner loop i.e., W_{in} and R_{in}. In double order NI-CG, there are six main parameters to be considered which include an element spacing (b), W_{out}, R_{out},W_{in}, R_{in} and the separation between two loops (L_s). In this work tewo types of NI-CGs have been utilized (1) NI-CG with chip resistors and (2) without chip resistors. The brief design description of these NI-CGs is as follows:

NI-CG without Resistors

The first and second order NI-CGs are shown in Figures 4.2(a) and (b). Each unit cell of CG used in the structure is having dimensions of 10 × 10mm with 0.5 mm boundary margin. These CG structures are impressed periodically on a dielectric substrate with relative permittivity ε_{r1}, loss tangent tan δ1 and thickness h1. A dielectric spacer is placed in between the CG and the ground plane with permittivity ε_{r2}, loss tangent tan δ2 and thickness h2. The ground plane used

in this paper should be conductive sheet as PEC with thickness H. The side view of the MMS is shown in figure 4.2(c) and the optimized dimensions are depicted in Table4.1.

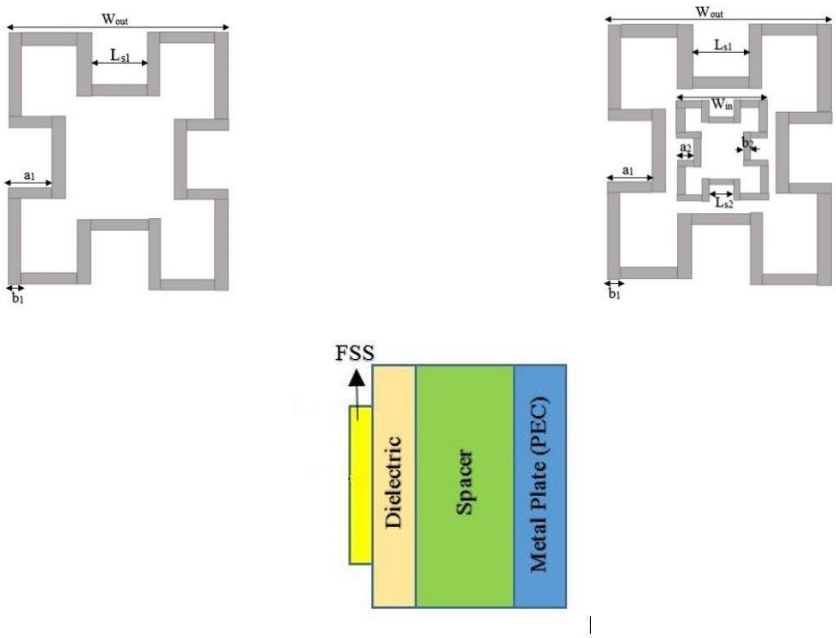

Figure 4.2. Unit cell geometry of the proposed MMS without resistors: (a) top views of First order CG, (b) Second Order CG (c) Side view

Resistor loaded NI-CGs

The unit cell geometry of first and Second order NI-CGs are illustrated in figures 4.3 (a) and (b). It consists of a top metallic structure imprinted on a thin dielectric substrate with relative permittivity ε_{r1}, loss tangent tan δ1 and thickness h1. A dielectric spacer is placed in between the CG and the ground plane with permittivity ε_{r2}, loss tangent tan δ2 and thickness h2. The top CG is built of single and double order NI-CG having split in the center of every arm of the loop. The lumped resistors are inserted at the split positions of every loop. Material1 is used as the dielectric substrate having dimensions mentioned previously. A dielectric spacer is placed between CG and the ground plane. The proposed design and corresponding design variables are depicted in Figure 4.3 and Table 4.1.

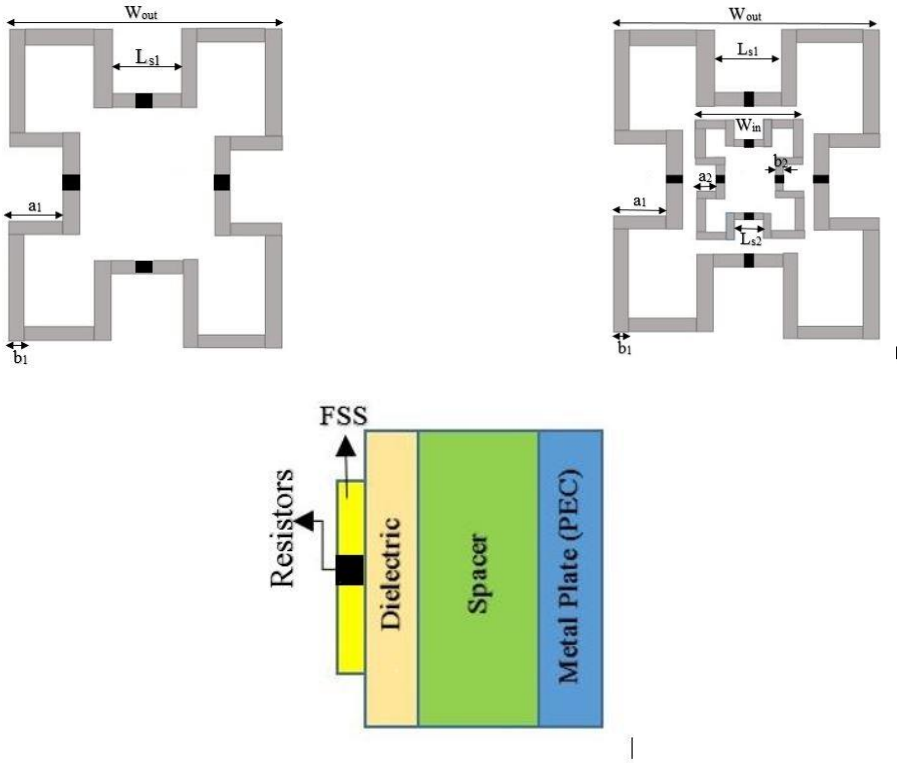

Figure 4.3. Unit cell geometry of the proposed MMS with resistors: (a) top views of First order CG, (b) Second Order CG (c) Side view

TABLE 4.1: OPTIMIZED DIMENSIONS

Parameters	Optimized values	Parameters	Optimized values
W_{out}	9.0 mm	εr2	1.05
W_{in}	4.2 mm	tan δ1	0.001
L_{S1}	3.0 mm	tan δ2	0.0017
L_{S2}	1.4 mm	H	2.0 mm
a1	1.5 mm	h1	0.8 mm
a2	0.7 mm	h2	3.8 mm
b1	0.5 mm	R_{in}	150 Ω
b2	0.2 mm	R_{out}	250 Ω
		εr1	2.25

4.3 RESULTS AND DISCUSSION

RL characteristics of NI-CG without resistors

Figure 4.4 shows the frequency dependent RL characteristics of first and second order NI-CG based MMSs without resistive elements. It has been observed that first order NI-CG achieve its peak RL value of -0.1 dB at the frequency at 4.6 GHz. On the other hand, when second order

NI-CG is considered, it possess resonant frequency at 10.4 GHz with the peak RL value of -1.2 dB.

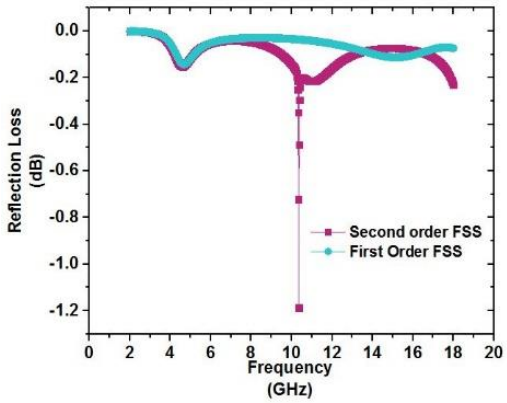

Figure 4.4. Frequency dependent RL characteristics of MMSs (a) First order CG and second order CG geometries based MMSs without resistive circuit elements.

Effect of the spacer on RL characteristics

The absorption bandwidth corresponding to RL ≤ -10 dB is the foremost requirement to achieve the good absorption characteristics. The incorporation of the spacer layer can improve the bandwidth of MMSs [35]. Therefore an effort has been made to examine the effect of the spacer thickness over the RL characteristics. An intact structure is developed adding the spacer (ε'=1.05 and tan δ=0.0017) in between the ground plane (PEC) and the dielectric substrate. The result shows that the reflectivity and resonance frequency can be changed by introducing the spacer as shown in Figure.4.5. Most importantly a tremendous enhancement has been observed in the -10 dB absorption bandwidth. The MMS structure with the spacer layer of thickness 3.8 mm has been found to provide a -10dB absorption bandwidth of 11.1 GHz (5.5-6.7 GHz). The peak RL value of -23.2 dB and it has been observed that there is a shift in the resonant frequency from higher to the lower frequency regimes.

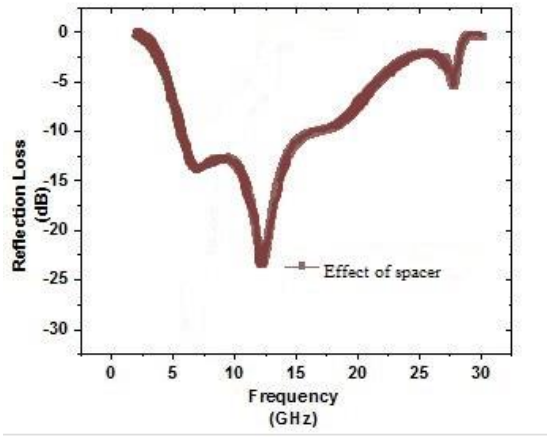

Figure 4.5. Frequency dependent characteristics showing the effect of the spacer in MMSs.

Effect of resistor incorporation over RL characteristics of NI- CGs

Figure. 4.6 shows the RL characteristics of resistor loaded first and second order NI-CG based MMSs. The absorption characteristics of second order NI-CG MMS are better than first order. A second order NI-CG MMS structure is found to accomplish more extensive peak RL value of – 23.1 dB at a frequency of 12.2 GHz with a wide bandwidth of 11.2 GHz (5.5- 16.7 GHz). Now the next step is to carry out a detailed analysis of second order NI-CGs in terms of their dielectric constant, substrate & spacer thickness and resistance value over absorption properties of MMS.

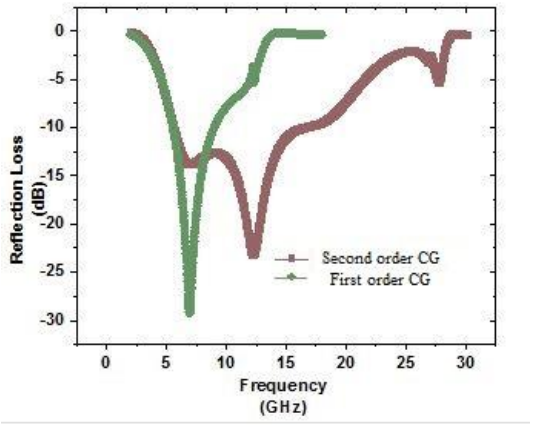

Figure 4.6.Frequency dependent RL characteristics of MMSs (a) First order NI- CG and second order NI- CG geometries based MMSs with resistive circuit elements.

RL characteristics of resistor loaded second order NI- CG MMSs

The critical analysis of RL characteristics of NI-CG MMS structure has been carried out using parametric analysis. In this section, three main aspects are primarily targeted such as (a). Effect

of the resistance variation, (b). Effect of the dielectric constant (c) Effect of the substrate thickness and (d) Effect of the spacer layer thickness on RL characteristics. In order to examine the effect of resistance insertion, two resistor R_{in}, R_{out} have been considered, where R_{out} is embedded in the outermost loop and R_{in} are incorporated in the inner loop as mentioned earlier in the design section. From the studies, it is observed that the RL characteristics can be controlled by changing the value of resistors [45].The RL characteristics of the MMS with variable resistance values of R_{out} and R_{in} are depicted in Figures 4.7(a) and (b), respectively. It has been observed that, as the value of the resistance varies, the RL characteristics are significantly enhanced. Moreover, the absorption bandwidth is broadened to the greatest extent with the bandwidth value of 11.1 GHz. Figure 4.7 (a) shows the RL characteristics of NI- CG based MMS where the resistance value of R_{out} is varied in the range of 150 to 450 Ω keeping R_{in} as constant. As the value of R_{out} varies it influence the RL characteristics of NI- CG MMSs. At R_{out} =250 Ω, the bandwidth of MMSs noticeably increased with the value of 11.1 GHz. Furthermore, the value of R_{in} is varied from 150 to 450 Ω keeping R_{out} constant as shown in the figure 4.7 (b), The improved RL characteristics have been achieved at an optimal resistance value of R_{in} =150 Ω with peak RL value of -23.1 dB at 12.2 GHz. From the above mentioned analysis, it can be concluded that enhanced RL characteristics and bandwidth are achieved by the resistors incorporated in the MMS.

The dielectric constant values have been varied in the range of 2 to 13. The substrates with ε′ =2.2 (Rogers), 5.9 (ferro), 10 (Arlon 1000) and 12.9 (Gallium Arsenide) have been chosen for the current study. The frequency dependent RL characteristics of NI- MMS with distinctive substrates are shown in figure 4.8 (a). It is clearly observed that the resonant frequencies decrease with the corresponding increase in the dielectric constant values. The resonance frequency and bandwidth of the NI- CG MMS decrease with increasing dielectric substrate constant. The lower dielectric substrate permittivity gives a higher value of electrical parameters of MMS. The MMS has a dielectric constant (ε′) value of 2.2 is found to provide broadband absorption characteristics as compared to the high dielectric constant substrate. The analyzed results of MMS for different values of substrate thickness (t) ranging from 0.8 to 3.2 mm is presented in figure 4.8 (b). It is seen that when t increases, absorption results get deteriorated.The optimized results observed shows the peak RL value of -23.1 dB at a frequency of 12.2 GHz with a bandwidth of 11.1 GHz (5.5 -16.7 GHz). From figure 4.8(c) it is clearly seen that when thickness increases from 1.8 to 3.8 mm. The resonating frequency changes accordingly and whole curve shifts towards the lower frequency end. It was clearly

observed that bandwidth has been increased to 11.1 GHz with RL value of -23.1 dB at 12.2 GHz.

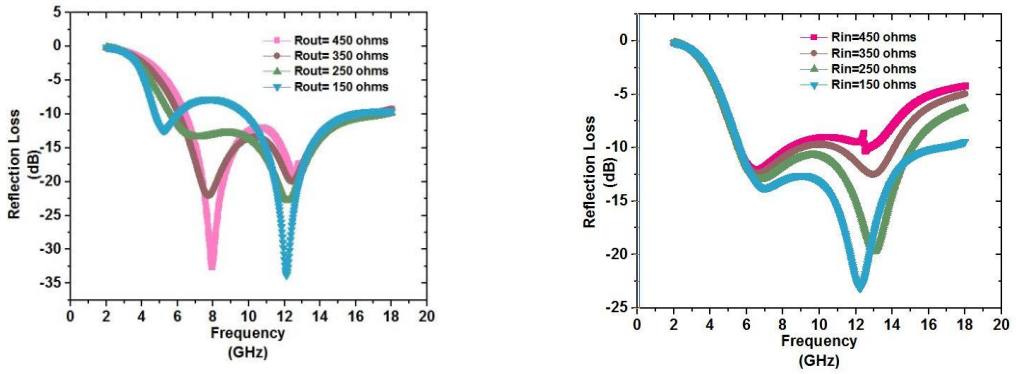

Figure 4.7. Frequency dependent RL characteristics of MMSs (a) Resistance of outer loop (R_{out}) is varied and (b). Resistance of inner loop (R_{in}) is varied

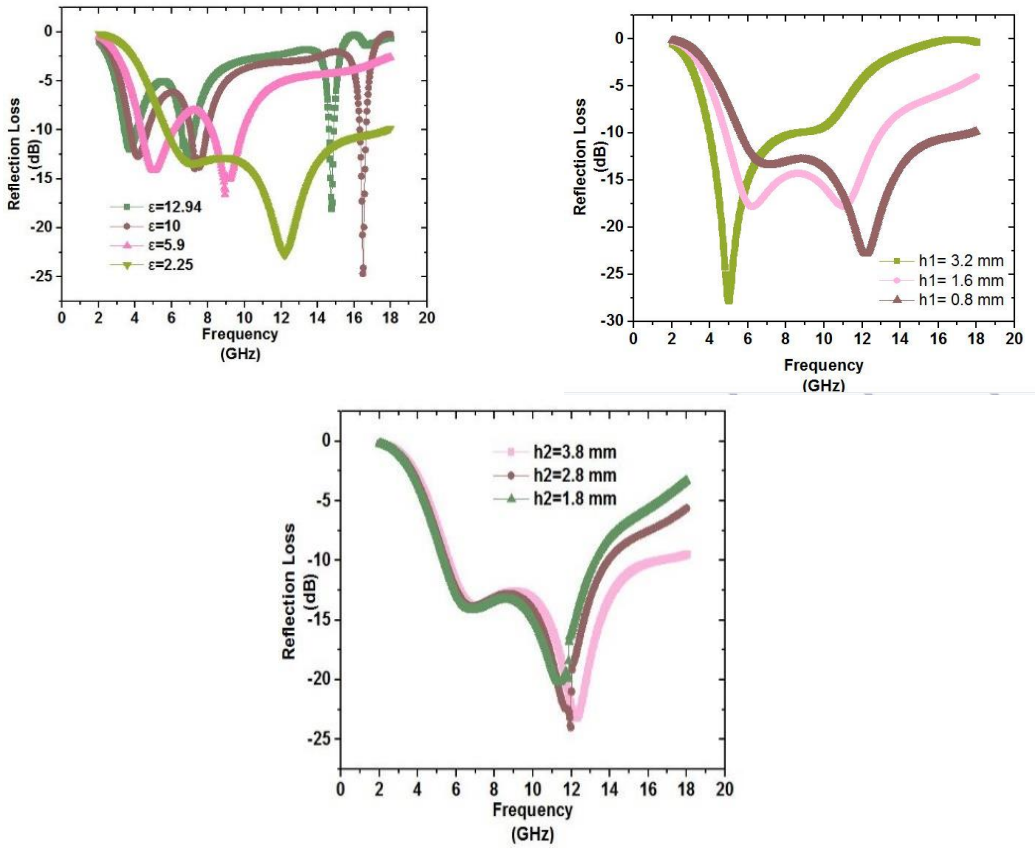

Figure 4.8. Simulated results of the 10x10 mm second order CG MMS vs. frequency for (a) Different dielectric constants ε′, (b) Different dielectric substrate thickness and (c) Different Spacer thickness

4.4 CONCLUSION

This chapter focuses on the designing of first and second order resistor loaded NI-CGs to enhance the RL characteristics. The detailed analysis on the parameters such as dielectric &spacer thickness, dielectric constant and resistance values were performed for the optimization of MMSs. A corresponding increase in the bandwidth has been observed with in a corresponding increase in an iteration order of CG. A NI-CG MMS structure is found to accomplish more extensive peak RL value of – 23.1 dB at a frequency of 12.2 GHz with a wide bandwidth of 11.2 GHz (5.5- 16.7 GHz). This study is beneficial for the future researchers to continue their work because this proposed MMS is able to achieve the minimum reflectivity and the wider bandwidth.

CHAPTER 5

CONCLUSION AND FUTURE SCOPE

5.1 CONCLUSION

In this thesis broadband MMSs were developed successfully by utilizing the concept of Resistor Loaded and Nature Inspired EM structures. It has been noticed that NI-CG provides a broadband frequency response, whereas TS-MMS, a type of traditional geometry when loaded with resistors provides an excellent RL characteristics. It is also observed that the design parameters such as dielectric & spacer thickness, dielectric constant and resistance values have a great impact on the RL characteristics of resistor loaded and nature inspired structures. A TS-MMS structure is found to accomplish more extensive peak RL value of - 14.5 dB at 6.2 GHz with wide bandwidth of 13. 0 GHz (4.9- 18.0 GHz). Similarly a NI-CG MMS structure is found to accomplish more extensive peak RL value of – 23.1 dB at a frequency of 12.2 GHz with a wide bandwidth of 11.2 GHz (5.5- 16.7 GHz). This study on MMS can be further utilized for numerous commercial applications like EMC, EMI and stealth technology and many more. The study carried out can provide a righteous platform for new researchers to continue their work in the same direction.

5.2 FUTURE SCOPE

- The studies carried out in this thesis were conducted in microwave regimes and in future the same can be achieved at millimeter and terahertz frequency regimes.
- The present studies were mainly focused towards the bandwidth of MMSs. Future studies may concentrate towards a possible elimination of the thickness-bandwidth trade-off.
- Only planar structures were considered under these studies. Nevertheless non planar structures such as tapered, curved, etc. can also be researched upon in the future.
- A non-destructive microwave measurement setup may be developed for evaluating the performance of the complex shaped EM structures.
- Only effect of resistor has been considered under studies, in the future the effect of diode such as PIN, IMPATT diodes, RF switches, Microelectromechanical systems (MEMS), Nanoelectromechanical systems (NEMS) etc. on RL characteristics of MMS can be studied.

REFRENCES

[1] Pryce,Imogen Mary,Resonant Metallic Nanostructures for Active Metamaterials and Photovoltaics,California Institute of Technology Pasadena, California 2011.

[2] Iyer,Ashwin K,Free-Space Metamaterial Superlenses using Transmission-Line Techniques,University of Toronto,2009.

[3] Rufangura,Patrick, Wide-Band Perfect Metamaterial Absorber For Solar Cell Applications,Middle Eat Technical University, 2015.

[4] Sood, Deepak, Design and characterization of compact ultra-thin metamaterial absorbers for narrowband and wideband RF applications, Kurukshetra University, 2014.

[5] Yan,Sen,Metamaterials Design and its Applications for Antennas, KU Leuven, Science, Engineering & Technology,2015.

[6] Bayatpur,Farhad,Metamaterial-Inspired Frequency-Selective Surfaces, The University of Michigan 2009.

[7] C. S. T. M. Studio, "CST Microwave studio," IEEE Microw. Mag., vol. 7, no. 4, pp. 11–11, 2006.

[8] Chip resistors. Available at https://www.digikey.com/products/en/resistors/chip-resistor-surface-mount/52.

[9] Fractal geometry design. Available at https://goo.gl/images/rHkN9i

[10] Sudhendra, C., Jose, P., Pillai, A. C. R., & Rao, K. (2014). Emerging Research in Electronics,Computer Science and Technology, 248.

[11] R. Panwar, S. Puthucheri, V. Agarwala, and D. Singh, "Fractal Frequency Selective Surface Embedded Thin Broadband Microwave Absorber Coatings Using Heterogeneous Composites," IEEE Trans. Microw. Theory Tech., vol. 63, no. 8, pp. 2438–2448, 2015.

[12] D. S. Wilbert, M. P. Hokmabadi, P. Kung, and S. M. Kim, "Equivalent-circuit interpretation of the polarization insensitive performance of THz metamaterial absorbers," IEEE Trans. Terahertz Sci. Technol., vol. 3, no. 6, pp. 846–850, 2013.

[13] Costa, F., Genovesi, S., Monorchio, A., & Manara, G. (2013). A circuit-based model For the interpretation of perfect metamaterial absorbers. IEEE Transactions on Antennas and Propagation, 61(3), 1201–1209.

[14] Zhang, L., Zhou, P., Zhang, H., Lu, L., Zhang, G., Chen, H., … Deng, L. (2014). A broadband radar absorber based on perforated magnetic polymer composites embedded with FSS. IEEE Transactions on Magnetics, 50(5).

[15] Ghosh, S., Member, S., & Bhattacharyya, S. (2015). An Ultra - wideband Ultra - thin Metamaterial Absorber Based on Circular Split Rings. IEEE Antennas and Wireless Propagation Letters, 1225, 1172–1175.

[16] Ghosh, S., Member, S., Srivastava, K. V., & Member, S. (2015). An Equivalent Circuit Model of FSS Based Metamaterial Absorber Using Coupled Line Theory, 14, 511–514.

[17] Lee, J., Yoo, M., & Lim, S. (2015). A study of ultra-thin single layer frequency selective surface microwave absorbers with three different bandwidths using double resonance. IEEE Transactions on Antennas and Propagation, 63(1), 221–230.

[18] Panwar, R., Puthucheri, S., Singh, D., & Agarwala, V. (2015). Design of Ferrite-Graphene-Based Thin Broadband Radar Wave Absorber for Stealth Application. IEEE

Transactions on Magnetics, 51(11), 12–15.
[19] Ghosh, S., & Srivastava, K. V. (2016). Polarization-insensitive single- and broadband switchable absorber/reflector and its realization using a novel biasing technique. IEEE Transactions on Antennas and Propagation, 64(8), 3665–3670.
[20] Unaldi, S., Cimen, S., Cakir, G., & Ayten, U. E. (2017). A Novel Dual-Band Ultrathin FSS With Closely Settled Frequency Response. IEEE Antennas and Wireless Propagation Letters, 16(c), 1381–1384.
[21] Panwar, R., & Lee, J. R. (2017). Progress in frequency selective surface-based smart electromagnetic structures: A critical review. Aerospace Science and Technology, 66(March), 216–234.
[22] Li, M. H., Liu, S. Y., Guo, L. Y., Lin, H., Yang, H. L., & Xiao, B. X. (2013). Influence of the dielectric-spacer thickness on the dual-band metamaterial absorber.Optics Communications, 295, 262–267.
[23] Li, S., Gao, J., Cao, X., Li, W., Zhang, Z., & Zhang, D. (2014). Wideband, thin, and polarization-insensitive perfect absorber based the double octagonal rings metamaterials and lumped resistances. Journal of Applied Physics, 116(4).
[24] Luo, Y., Zhuang, Y., & Zhu, S. (2009). Thin and broadband Salisbury screen absorber using Minkowski fractal structure. APMC 2009 - Asia Pacific Microwave Conference 2009, 2573–2576.
[25] Costa, F., Monorchio, A., & Manara, G. (2010). Analysis and design of ultra thin electromagnetic absorbers comprising resistively loaded high impedance surfaces.IEEE Transactions on Antennas and Propagation, 58(5), 1551–1558.
[26] Taylor, P. S., Parker, E. A., & Batchelor, J. C. (2011). An active annular ring frequency selective surface. IEEE Transactions on Antennas and Propagation, 59(9), 3265–3271.
[27] Li, J., Jiang, J., He, Y., Xu, W., Chen, M., Miao, L., & Bie, S. (2015). Design of a Tunable Low - Frequency and Broadband Radar Absorber Based on Active Frequency Selective Surface. IEEE Antennas and Wireless Propagation Letters, 1225(d), 8–11.
[28] Fan, Y., Zhang, H. C., Yin, J. Y., Xu, L., Nagarkoti, D. S., Hao, Y., & Cui, T. J. (2016). An Active Wideband and Wide-Angle Electromagnetic Absorber at Microwave Frequencies. IEEE Antennas and Wireless Propagation Letters, 15, 1913–1916.
[29] Yang, J., & Shen, Z. (2007). A thin and broadband absorber using double-square loops. IEEE Antennas and Wireless Propagation Letters, 6, 388–391.
[30] Ford, K. L., Holtby, D. G., & Chambers, B. (2009). Optimisation of a pyramidal geometric transition radar absorbing material loaded with a resistive frequency selective surface. Iet Radar Sonar and Navigation, 3(6), 596–600.
[31] Liao, Z., Gong, R., Nie, Y., Wang, T., & Wang, X. (2011). Absorption enhancement of fractal frequency selective surface absorbers by using microwave absorbing material based substrates. Photonics and Nanostructures - Fundamentals and Applications, 9(3).
[32] Panwar, R., Puthucheri, S., Singh, A., Singh, D., & Agarwala, V. (2015). Critical Analysis of Fractal FSS with Heterogeneous Composite to Enhance Microwave Absorption for Stealth Application, 416–418.
[33] Zhao, Z., Shi, H., Guo, J., Li, W., & Zhang, A. (2017). Stopband Frequency Selective Surface With Ultra-Large Angle of Incidence. IEEE Antennas and Wireless Propagation Letters, 16, 553–556.
[34] Popržen, N., & Gaćanović, M. (n.d.). Fractal Antennas : Design , Characteristics and

Application. Fractals An Interdisciplinary Journal On The Complex Geometry Of Nature.
[35] Romeu, J., & Rahmat-Samii, Y. (2000). Fractal FSS: a novel dual-band frequency selective surface. IEEE Transactions on Antennas and Propagation, 48(7), 1097– 1105.
[36] Gianvittorio, J. P., Romeu, J., Blanch, S., & Rahmat-Samii, Y. (2003). Self-Similar Prefractal Frequency Selective Surfaces for Multiband and Dual-Polarized Applications. IEEE Transactions on Antennas and Propagation, 51(11), 3088–3096.
[37] Ghosh, S., Bhattacharyya, S., & Srivastava, K. V. (2017). Design and analysis of a broadband single layer circuit analog absorber. European Microwave Week 2016: "Microwaves Everywhere", EuMW 2016 - Conference Proceedings; 46th European Microwave Conference, EuMC 2016, 584–587.
[38] Wang, T., Wang, L., Nie, Y., & Gong, R. (2010). Relation between dielectric spacer thickness and absorption feature in metamaterials absorber. Conference Proceedings of the International Symposium on Signals, Systems and Electronics, 1, 31–34.
[39] Li, J., Jiang, J., He, Y., Xu, W., Chen, M., Miao, L., & Bie, S. (2015). Design of a Tunable Low - Frequency and Broadband Radar Absorber Based on Active Frequency Selective Surface.IEEE Antennas and Wireless Propagation Letters, 1225(d), 8–11.
[40] Xu, H., Bie, S., Jiang, J., Wan, D., Zhou, J., & Xu, Y. (2014). Broadening bandwidth of the composite radar absorption material involving a frequency selective surface. Journal of Electromagnetic Waves and Applications, (January 2015), 1–9.
[41] Munk, B. E. N. A. (n.d.). SURFACES FREQUENCY SELECTIVE Theory and Design,The Ohio State University, 2000
[42] Ghosh, S., Bhattacharyya, S., & Srivastava, K. V. (2017). Design and analysis of a broadband single layer circuit analog absorber. European Microwave Week 2016: "Microwaves Everywhere", EuMW 2016 - Conference Proceedings; 46th European Microwave Conference, EuMC 2016, 584–587.
[43] Hartog, A. H., Payne, D. N., Baptista, J. M., Santos, J. L., Falate, R., Baptista, J. M., Mir- , F. L. (2016). AN ULTRA THIN POLARIZATION INSENSITIVE AND ANGULARLY STABLE MINIATURIZED FREQUENCY SELECTIVE, 58(11), 2713 2717.
[44] Bandyopadhyay, A. K., Delhi, N., Sharma, S. K., Ghosh, S., Srivastava, K. V., & Shukla, A. (2017). ULTRA-THIN DUAL-BAND CONFORMAL METAMATERIAL, 59(2), 1344–1345.

LIST OF PUBLICATIONS

[1] T.K. Suchu, R. Panwar, R. Khanna, 'Design of lumped resistor based broadband metamaterial structure from 2 to 18 GHz', META07 International Conference of Metamaterials (META07), South Korea, July 25-28, 2017 **(Accepted**).

[2] T.K. Suchu, R. Panwar, R. Khanna, Design and analysis of resistor loaded square aperture geometry based broadband metamaterial structure, International Journal of Electromagnetics (Taylor & Francis), 2017 (**Communicated**).

[3] T.K. Suchu, R. Panwar, R. Khanna, Design and analysis of nature inspired geometry based broadband metamaterial structure, 2017 (**Under preparation**).